Physics Letters B 765 (2017) 193–220

Contents lists available at ScienceDirect

Physics Letters B

www.elsevier.com/locate/physletb

Evidence for collectivity in pp collisions at the LHC

The CMS Collaboration *

CERN, Switzerland

ARTICLE INFO

Article history:
Received 20 June 2016
Received in revised form 3 December 2016
Accepted 5 December 2016
Available online 13 December 2016
Editor: M. Doser

Keywords:
CMS
Physics
Heavy ion
Ridge
Correlation
pp

ABSTRACT

Measurements of two- and multi-particle angular correlations in pp collisions at $\sqrt{s} = 5$, 7, and 13 TeV are presented as a function of charged-particle multiplicity. The data, corresponding to integrated luminosities of 1.0 pb^{-1} (5 TeV), 6.2 pb^{-1} (7 TeV), and 0.7 pb^{-1} (13 TeV), were collected using the CMS detector at the LHC. The second-order (v_2) and third-order (v_3) azimuthal anisotropy harmonics of unidentified charged particles, as well as v_2 of K^0_S and $\Lambda/\overline{\Lambda}$ particles, are extracted from long-range two-particle correlations as functions of particle multiplicity and transverse momentum. For high-multiplicity pp events, a mass ordering is observed for the v_2 values of charged hadrons (mostly pions), K^0_S, and $\Lambda/\overline{\Lambda}$, with lighter particle species exhibiting a stronger azimuthal anisotropy signal below $p_T \approx 2$ GeV/c. For 13 TeV data, the v_2 signals are also extracted from four- and six-particle correlations for the first time in pp collisions, with comparable magnitude to those from two-particle correlations. These observations are similar to those seen in pPb and PbPb collisions, and support the interpretation of a collective origin for the observed long-range correlations in high-multiplicity pp collisions.

1. Introduction

The observation of long-range two-particle azimuthal correlations at large relative pseudorapidity ($|\Delta\eta|$) in high final-state particle multiplicity (high-multiplicity) proton–proton (pp) [1–3] and proton–lead (pPb) [4–7] collisions at the LHC has opened up new opportunities for studying novel dynamics of particle production in small, high-density quantum chromodynamic (QCD) systems. A key feature of such correlations is an enhanced structure on the near side (relative azimuthal angle $|\Delta\phi| \approx 0$) of two-particle $\Delta\eta$–$\Delta\phi$ correlation functions that extends over a wide range in relative pseudorapidity ($|\Delta\eta| \approx 4$). Such a long-range, near side correlation structure, known as the "ridge", was first observed in relativistic nucleus–nucleus (AA) collisions from RHIC to LHC energies, including copper–copper [8], gold–gold [8–12], and lead–lead (PbPb) [13–18] systems. Based on extensive studies, it has been suggested that the hydrodynamic collective flow of a strongly interacting and expanding medium [19–21] is responsible for these long-range correlations in these large heavy ion systems. In hydrodynamic models, the detailed azimuthal correlation structure of emitted particles is typically characterized by its Fourier components [22]. In particular, the second and third Fourier components, known as elliptic (v_2) and triangular (v_3) flow, most directly reflect the medium response to, respectively, the initial collision geometry and its fluctuations [23], providing insight into fundamental transport properties of the medium [24–26]. Recently, at RHIC, such long-range correlations have also been observed and studied in lighter AA systems such as dAu [27,28] and ^{3}HeAu [29].

In systems such as pp and pPb, where the transverse size of the overlap region is comparable to that of a single proton, the formation of a hot and dense fluid-like medium was not expected. The expectations for other small systems like dAu and ^{3}HeAu were similar. Various theoretical models have been proposed to interpret the origin of the observed long-range correlations in small collision systems [30–37]. These include initial-state gluon correlations without final-state interactions [33,34] or, similar to what is thought to occur in AA systems, hydrodynamic flow that develops in a conjectured high-density medium [35–37].

Owing to the magnitude of the correlation signal, significant progress has been made in unraveling the nature of the ridge correlations in high-multiplicity pPb collisions. Measurements of anisotropy Fourier harmonics (v_n), using identified particles [38,39] and multi-particle correlation techniques [40–43], reveal features that support a collective origin of the observed correlations [44–47].

In high-multiplicity pp collisions, the nature of the observed long-range correlation still remains poorly understood. Long-range correlations in pp collisions were first observed at $\sqrt{s} = 7$ TeV [1], and the extraction of anisotropy v_2 harmonics in pp collisions was

* *E-mail address:* cms-publication-committee-chair@cern.ch.

http://dx.doi.org/10.1016/j.physletb.2016.12.009

recently reported using data at $\sqrt{s} = 13\,\text{TeV}$ [2]. A better understanding of the underlying particle correlation mechanisms leading to these observations requires more detailed study of the properties of the v_2 and higher-order harmonics in pp collisions. In particular, their dependence on particle species, and other aspects related to their possible collective nature, are the key to scrutinize various theoretical interpretations. Furthermore, a quantitative modeling of long-range correlations in pPb collisions is found to be highly sensitive to the spatial structure of the proton [35]. Fluctuations of the substructure of nucleons are not well understood, but they can be better constrained with studies of anisotropy harmonics in pp collisions.

This paper extends the characterization of long-range correlation phenomena in high-multiplicity pp collisions by presenting a detailed study of two- and multi-particle azimuthal correlations with unidentified charged particles, as well as correlations of reconstructed K^0_S and $\Lambda/\overline{\Lambda}$ particles at various LHC collision energies. The results of v_2 and v_3 harmonics, extracted from two-particle correlations, are studied as functions of particle p_T and event multiplicity. The residual contribution to long-range correlations of back-to-back jet correlations is estimated and removed by subtracting correlations obtained from very low multiplicity pp events. The v_2 harmonics are also extracted using the multi-particle cumulant method to shed light on the possible collective nature of the correlations. The pp results are directly compared to those found for pPb and PbPb systems over a broad range of similar multiplicities.

2. The CMS detector and data sets

The central feature of the CMS apparatus is a superconducting solenoid of 6 m internal diameter. Within the solenoid volume, there are a silicon pixel and strip tracker detector, a lead tungstate crystal electromagnetic calorimeter (ECAL), and a brass and scintillator hadron calorimeter (HCAL), each composed of a barrel and two endcap sections. Muons are measured in gas-ionization detectors embedded in the steel flux-return yoke outside the solenoid. The silicon tracker measures charged particles within the pseudorapidity range $|\eta| < 2.5$. It consists of 1440 silicon pixel and 15 148 silicon strip detector modules and is located in the 3.8 T field of the solenoid. For non-isolated particles of $1 < p_\mathrm{T} < 10\,\text{GeV}/c$ and $|\eta| < 1.4$, the track resolutions are typically 1.5% in p_T and 25–90 (45–150) μm in the transverse (longitudinal) impact parameter [48]. Iron and quartz-fiber Cherenkov hadron forward (HF) calorimeters cover the range $2.9 < |\eta| < 5.2$ on either side of the interaction region. These HF calorimeters are azimuthally subdivided into 20° modular wedges and further segmented to form $0.175 \times 0.175\,\text{rad}^2$ ($\Delta\eta \times \Delta\phi$) "towers". The beam pickup for timing (BPTX) devices is designed to provide precise information on the LHC bunch structure and timing of the incoming beams. They are located around the beam pipe at a distance of 175 m from the interaction point on either side. A more detailed description of the CMS detector, together with a definition of the coordinate system used and the relevant kinematic variables, can be found in Ref. [49]. The detailed Monte Carlo (MC) simulation of the CMS detector response is based on GEANT4 [50].

The data samples of pp collisions used in this analysis were collected by the CMS experiment in 2010 at $\sqrt{s} = 7\,\text{TeV}$, and in 2015 at 5.02 TeV (labeled as 5 TeV for simplicity) and 13 TeV, with integrated luminosities of 6.2, 1.0, and $0.7\,\text{pb}^{-1}$, respectively.

3. Event and track selection

Minimum bias (MB) pp events were triggered by requiring the coincidence of signals from both BPTX devices, indicating the presence of two proton bunches crossing at the interaction point (zero bias condition). The data used in this study were recorded with an average number of pp interactions per bunch crossing ranging from 0.1 to 1.4. Because of hardware limits on the data acquisition rate, only a small fraction ($\sim 10^{-3}$) of all MB triggered events were recorded. In order to collect a large sample of high-multiplicity pp collisions, a dedicated trigger was implemented using the CMS level-1 (L1) and high-level trigger (HLT) systems. At L1, the total transverse energy summed over ECAL and HCAL was required to be greater than a given threshold (40, 45 and 55 GeV thresholds are used). Online track reconstruction for the HLT was based on the three layers of pixel detectors, requiring the track origin to be located within a cylindrical region centered on the nominal interaction point with a length of 30 cm along the beam and a radius of 0.2 cm perpendicular to the beam. For each event, the vertex reconstructed with the highest number of pixel tracks was selected. The vertex reconstruction efficiency with high track multiplicities is 100%. The number of pixel tracks ($N_\mathrm{trk}^\mathrm{online}$) with $|\eta| < 2.4$, $p_\mathrm{T} > 0.4\,\text{GeV}/c$, and a distance of closest approach less than 0.12 cm to this vertex, was determined for each event. Data were taken with HLT thresholds of $N_\mathrm{trk}^\mathrm{online} \geq 60$, 85, 110, seeded with L1 total transverse energy thresholds of 40, 45, and 55 GeV, respectively.

In the offline analysis, hadronic collisions are selected by requiring at least one HF calorimeter tower with more than 3 GeV of total energy in each of the two HF detectors. Events are also required to contain at least one reconstructed primary vertex within 15 cm of the nominal interaction point along the beam axis and within 0.15 cm in the direction transverse to the beam trajectory. Beam related background is suppressed by rejecting events for which less than 25% of all reconstructed tracks pass the *high-purity* selection (as defined in Ref. [48]). With these selection criteria, 94–96% of the pp interactions simulated with PYTHIA 6 tune Z2 [51] and PYTHIA 8 tune CUETP8M1 [52] event generators that have at least one particle with energy $E > 3\,\text{GeV}$ in both ranges $-5 < \eta < -3$ and $3 < \eta < 5$ are selected.

In this analysis, primary tracks, i.e. tracks that emanate from the primary vertex and that satisfy the high-purity criteria, are used to define the event charged-particle multiplicity and perform correlation measurements. Additional requirements are also applied to enhance the purity of primary tracks. The significance of the separation along the beam axis (z) between the track and the primary vertex, $d_z/\sigma(d_z)$, and the significance of the impact parameter relative to the primary vertex transverse to the beam, $d_\mathrm{T}/\sigma(d_\mathrm{T})$, must be smaller than 3. The relative uncertainty of the transverse-momentum measurement, $\sigma(p_\mathrm{T})/p_\mathrm{T}$, must be smaller than 10%. To ensure high tracking efficiency and to reduce the rate of misreconstructed tracks, only tracks in the region $|\eta| < 2.4$ and $p_\mathrm{T} > 0.3\,\text{GeV}/c$ are included. The p_T threshold is raised to $0.4\,\text{GeV}/c$ for purposes of the event multiplicity determination, to match the requirement in the HLT, while tracks down to $0.3\,\text{GeV}/c$ are used in the correlation analysis. Based on simulation studies using GEANT4 to propagate particles from the PYTHIA 8 event generator, the combined geometrical acceptance and efficiency for primary track reconstruction exceeds 60% for $p_\mathrm{T} \approx 0.3\,\text{GeV}/c$ and $|\eta| < 2.4$. The efficiency is greater than 90% in the $|\eta| < 1$ region for $p_\mathrm{T} > 0.6\,\text{GeV}/c$. For the event multiplicity range studied in this paper, no dependence of the tracking efficiency on the multiplicity is found and the rate of misreconstructed tracks is 1–2%.

Additionally, the CMS *loose* [48] tracks are also used to incorporate secondary-track candidates with larger track impact parameters, for reconstructing K^0_S and $\Lambda/\overline{\Lambda}$ candidates (also called V^0 candidates). The reconstruction of V^0 candidates in this analysis is identical to that in Refs. [39,53], where more details can be found. Oppositely charged tracks that are detached (having large

Table 1
Fraction of MB triggered events after event selections in each multiplicity bin, and the average multiplicity of reconstructed tracks per bin with $|\eta| < 2.4$ and $p_T > 0.4\,\text{GeV}/c$, before ($N_{\text{trk}}^{\text{offline}}$) and after ($N_{\text{trk}}^{\text{corrected}}$) efficiency correction, for pp data at $\sqrt{s} = 5$, 7, and 13 TeV.

$N_{\text{trk}}^{\text{offline}}$	Fraction			$\langle N_{\text{trk}}^{\text{offline}} \rangle$			$\langle N_{\text{trk}}^{\text{corrected}} \rangle$		
	5 TeV	7 TeV	13 TeV	5 TeV	7 TeV	13 TeV	5 TeV	7 TeV	13 TeV
MB	1.0	1.0	1.0	13	15	16	16 ± 1	17 ± 1	19 ± 1
[0, 10)	0.48	0.44	0.43	4.8	4.8	4.8	5.8 ± 0.3	5.5 ± 0.2	5.9 ± 0.3
[10, 20)	0.29	0.28	0.26	14	14	14	17 ± 1	16 ± 1	17 ± 1
[20, 30)	0.14	0.15	0.15	24	24	24	28 ± 1	28 ± 1	30 ± 1
[30, 40)	0.06	0.08	0.08	34	34	34	41 ± 2	40 ± 2	42 ± 2
[40, 60)	0.03	0.05	0.07	47	47	47	56 ± 2	54 ± 2	58 ± 2
[60, 85)	3×10^{-3}	7×10^{-3}	0.02	66	67	68	80 ± 3	78 ± 3	83 ± 3
[85, 95)	9×10^{-5}	3×10^{-4}	1×10^{-3}	88	89	89	106 ± 4	103 ± 4	109 ± 4
[95, 105)	2×10^{-5}	9×10^{-5}	5×10^{-4}	98	99	99	118 ± 5	114 ± 4	121 ± 5
[105, 115)	5×10^{-6}	2×10^{-5}	2×10^{-4}	108	109	109	130 ± 5	126 ± 5	133 ± 5
[115, 125)	1×10^{-6}	8×10^{-6}	6×10^{-5}	118	118	119	142 ± 6	137 ± 5	145 ± 6
[125, 135)	2×10^{-7}	2×10^{-6}	2×10^{-5}	126	128	129	153 ± 6	149 ± 6	157 ± 6
[135, 150)	5×10^{-8}	4×10^{-7}	8×10^{-6}	139	140	140	167 ± 7	162 ± 6	171 ± 7
[150, ∞)	5×10^{-9}	8×10^{-8}	2×10^{-6}	155	156	158	186 ± 8	181 ± 7	193 ± 8

$d_z/\sigma(d_z)$ and $d_T/\sigma(d_T)$ values) from the primary vertex are selected to determine if they point to a common secondary vertex. The pair of tracks are assumed to be $\pi^+\pi^-$ in K_S^0 reconstruction, while the assumption of $\pi^-\text{p}(\pi^+\overline{\text{p}})$ is used in Λ ($\overline{\Lambda}$) reconstruction. The angle θ^{point} between the V^0 momentum vector and the vector connecting the primary and V^0 vertices is required to satisfy $\cos(\theta^{\text{point}}) > 0.999$. The K_S^0 ($\Lambda/\overline{\Lambda}$) reconstruction efficiency is about 6% (1%) for $p_T \approx 1\,\text{GeV}/c$ and 17%(7%) for $p_T > 3\,\text{GeV}/c$ within $|\eta| < 2.4$. This efficiency includes the effects of acceptance and the branching ratio for V^0 particle decays into neutral particles. The relatively low reconstruction efficiency of the V^0 candidates is primarily due to the low efficiency for reconstructing daughter tracks with $p_T < 0.3\,\text{GeV}/c$ or larger impact parameters.

Following the same procedure as used in previous analyses [1,4,43], the pp data sets at different energies are divided into classes of reconstructed track multiplicity, $N_{\text{trk}}^{\text{offline}}$, where primary tracks with $|\eta| < 2.4$ and $p_T > 0.4\,\text{GeV}/c$ are counted. Details of the multiplicity classification in this analysis, including the fractional inelastic cross section and the average number of primary tracks before and after correcting for detector effects in each multiplicity range, are provided in Table 1. Within a given $N_{\text{trk}}^{\text{offline}}$ range, the average event multiplicity is expected to be larger for higher $\sqrt{s}$ data, as suggested by the average uncorrected $N_{\text{trk}}^{\text{offline}}$ values. However, due to a slightly higher tracking efficiency, and hence a smaller efficiency correction, the corrected average multiplicity, $N_{\text{trk}}^{\text{corrected}}$, for the same $N_{\text{trk}}^{\text{offline}}$ range happens to be smaller for 7 TeV data than for 5 TeV data. Uncertainties on $N_{\text{trk}}^{\text{corrected}}$ values come from systematic uncertainties on the tracking efficiency correction factor estimated from MC simulations.

4. Analysis technique

The analysis techniques for two- and multi-particle correlations are identical to those used in Refs. [3,4,13,14,39,40,43]. They are briefly summarized in this section for the analysis of the new pp data samples.

4.1. Two-particle correlations and Fourier harmonics

For each track multiplicity class, "trigger" particles are defined as charged particles or V^0 candidates with $|\eta| < 2.4$ and originating from the primary vertex within a given p_T^{trig} range. The number of trigger particles in the event is denoted by N_{trig}. Particle pairs are then formed by associating each trigger particle with the remaining charged primary tracks with $|\eta| < 2.4$ and from a specified p_T^{assoc} interval (which can be either the same as or different from the p_T^{trig} range). A pair is removed if the associated particle is the daughter of any trigger V^0 candidate (this contribution is negligible since associated particles are mostly primary tracks). The two-dimensional (2D) per-trigger-particle associated yield is defined in the same way as done in previous analyses,

$$\frac{1}{N_{\text{trig}}}\frac{\text{d}^2N^{\text{pair}}}{\text{d}\Delta\eta\,\text{d}\Delta\phi} = B(0,0)\,\frac{S(\Delta\eta,\Delta\phi)}{B(\Delta\eta,\Delta\phi)}, \tag{1}$$

where $\Delta\eta$ and $\Delta\phi$ are the differences in η and ϕ of the pair. The same-event pair distribution, $S(\Delta\eta,\Delta\phi)$, represents the yield of particle pairs normalized by N_{trig} from the same event,

$$S(\Delta\eta,\Delta\phi) = \frac{1}{N_{\text{trig}}}\frac{\text{d}^2N^{\text{same}}}{\text{d}\Delta\eta\,\text{d}\Delta\phi}. \tag{2}$$

The mixed-event pair distribution,

$$B(\Delta\eta,\Delta\phi) = \frac{1}{N_{\text{trig}}}\frac{\text{d}^2N^{\text{mix}}}{\text{d}\Delta\eta\,\text{d}\Delta\phi}, \tag{3}$$

is constructed by pairing the trigger particles in each event with the associated charged particles from 20 different randomly selected events in the same 0.5 cm wide z_{vtx} range and from the same track multiplicity class. The same-event and mixed-event pair distributions are first calculated for each event, and then averaged over all the events within the track multiplicity class. The ratio $B(0,0)/B(\Delta\eta,\Delta\phi)$ mainly accounts for pair acceptance effects, with $B(0,0)$ representing the mixed-event associated yield for both particles of the pair going in approximately the same direction and thus having maximum pair acceptance. Following the procedure described in Refs. [4,13,14,39,43], each reconstructed primary track and V^0 candidate is weighted by a correction factor derived from MC simulations, which accounts for detector effects including the reconstruction efficiency, the detector acceptance, and the fraction of misreconstructed tracks.

The azimuthal anisotropy harmonics of charged particles, K_S^0 and $\Lambda/\overline{\Lambda}$ particles can be extracted via a Fourier decomposition of long-range two-particle $\Delta\phi$ correlation functions, obtained by averaging the 2D two-particle correlation function over $|\Delta\eta| > 2$ (to remove short-range correlations, such as those from jet fragmentation),

$$\frac{1}{N_{\text{trig}}}\frac{\text{d}N^{\text{pair}}}{\text{d}\Delta\phi} = \frac{N_{\text{assoc}}}{2\pi}\left[1 + \sum_n 2V_{n\Delta}\cos(n\Delta\phi)\right], \tag{4}$$

where $V_{n\Delta}$ are the Fourier coefficients and $N_{\rm assoc}$ represents the average number of pairs per trigger particle for a given $(p_{\rm T}^{\rm trig}, p_{\rm T}^{\rm assoc})$ bin. The first three Fourier terms are included in the fits to the dihadron correlation functions. Including additional terms has a negligible effect on the results of the Fourier fit.

Assuming $V_{n\Delta}$ coefficients can be factorized into the product of single-particle anisotropies [43], the elliptic and triangular anisotropy harmonics, $v_2\{2, |\Delta\eta| > 2\}$ and $v_3\{2, |\Delta\eta| > 2\}$, of trigger particles can be extracted as a function of $p_{\rm T}$ from the fitted Fourier coefficients from the two-particle correlation method,

$$v_n(p_{\rm T}^{\rm trig}) = \frac{V_{n\Delta}(p_{\rm T}^{\rm trig}, p_{\rm T}^{\rm ref})}{\sqrt{V_{n\Delta}(p_{\rm T}^{\rm ref}, p_{\rm T}^{\rm ref})}}, \qquad n = 2, 3. \tag{5}$$

Here, a fixed $p_{\rm T}^{\rm ref}$ range for the "reference" charged primary particles is chosen to be $0.3 < p_{\rm T} < 3.0\,{\rm GeV}/c$ to minimize correlations from jets at higher $p_{\rm T}$.

To extract v_2 signal for V^0 candidates, the invariant mass distributions are fitted by a sum of two Gaussian functions with a common mean to describe the true V^0 signal peak, and a fourth-order polynomial function to model the background, as done in Ref. [39]. The v_2 values are first extracted for V^0 candidates from the peak region (which contains contributions from genuine V^0, as well as background V^0 candidates from random combinatorics) and from a sideband region (which contains only background V^0s from random combinatorics), denoted as $v_2^{\rm obs}$ and $v_2^{\rm bkg}$. Here the peak region is defined as the mass window of $\pm 2\sigma$ around the center of the V^0 candidate mass peak, where σ is found from the addition in quadrature of the standard deviations of the two Gaussian functions weighted by their yields. The sideband region is defined as the mass window outside $\pm 3\sigma$ mass range around the V^0 candidate mass peak to upper limit of $0.565\,(1.135)\,{\rm GeV}$ and lower limit of $0.430\,(1.155)\,{\rm GeV}$ for $\rm K^0_S$ ($\Lambda/\overline{\Lambda}$) particles. The v_2 signal for V^0 candidates can then be calculated as

$$v_2^{\rm sig} = \frac{v_2^{\rm obs} - (1 - f^{\rm sig})\, v_2^{\rm bkg}}{f^{\rm sig}}, \tag{6}$$

where $f^{\rm sig}$ represents the signal yield fraction in the peak region determined from the fits to the mass distribution. This fraction exceeds 80% for $\Lambda/\overline{\Lambda}$ candidates with $p_{\rm T} > 1\,{\rm GeV}/c$ and is above 95% for $\rm K^0_S$ candidates over the entire $p_{\rm T}$ range.

Although a requirement of $|\Delta\eta| > 2$ can largely exclude near side jet-like correlations for $v_n\{2\}$ extraction, contributions from back-to-back (i.e. dijet) correlations are still present in the long-range, away side ($\Delta\phi \approx \pi$) region, especially for pp collisions. By assuming that the shape of the jet-induced correlations is invariant with event multiplicity, a procedure of removing jet-like correlations in pPb collisions was proposed in Refs. [5,6]. The method consists of subtracting the results for low-multiplicity events, where the ridge signal is not present, from those for high-multiplicity events. For this analysis, a very similar low-multiplicity subtraction method developed for pPb collisions [43] is employed. The Fourier coefficients, $V_{n\Delta}$, extracted from Eq. (4) for $10 \le N_{\rm trk}^{\rm offline} < 20$ are subtracted from the $V_{n\Delta}$ coefficients extracted in the higher-multiplicity region, with

$$\begin{aligned} V_{n\Delta}^{\rm sub} = {} & V_{n\Delta} - V_{n\Delta}(10 \le N_{\rm trk}^{\rm offline} < 20) \\ & \times \frac{N_{\rm assoc}(10 \le N_{\rm trk}^{\rm offline} < 20)}{N_{\rm assoc}} \\ & \times \frac{Y_{\rm jet}}{Y_{\rm jet}(10 \le N_{\rm trk}^{\rm offline} < 20)}. \end{aligned} \tag{7}$$

Here, $Y_{\rm jet}$ represents the near side jet yield obtained by integrating the difference of the short- and long-range event-normalized associated yields for each multiplicity class as shown for $105 \le N_{\rm trk}^{\rm offline} < 150$ in Fig. 2 (to be described in Section 5.1) over $|\Delta\phi| < 1.2$. The ratio, $Y_{\rm jet}/Y_{\rm jet}(10 \le N_{\rm trk}^{\rm offline} < 20)$, is introduced to account for the enhanced jet correlations resulting from the selection of higher-multiplicity events. This jet subtraction procedure is verified using PYTHIA 6 (Z2) and PYTHIA 8 tune CUETP8M1 pp simulations, where no jet modification from initial- or final-state effects is present. The residual $V_{n\Delta}$ after subtraction is found to be consistent with zero. The azimuthal anisotropy harmonics v_n after correcting for back-to-back jet correlations estimated from low-multiplicity data (denoted as $v_n^{\rm sub}$) can be extracted from $V_{n\Delta}^{\rm sub}$ using Eq. (5) and (6). In this paper, both the v_n and $v_n^{\rm sub}$ results are presented.

4.2. Fourier harmonics from multi-particle correlations

To avoid a model-dependent correction of jet-like correlations in extracting v_n harmonics from two-particle correlations, a multi-particle cumulant analysis using the Q-cumulant method [54] is employed to determine the second-order elliptic harmonic, similar to what was done in pPb and PbPb collisions [40,43]. By simultaneously correlating several (no less than four) particles, the multi-particle cumulant technique has the advantage of suppressing short-range two-particle correlations such as jets and resonance decays. It also serves as a powerful tool to directly probe the collective nature of the observed azimuthal correlations.

The two-, four-, and six-particle azimuthal correlations [54] are evaluated as:

$$\begin{aligned} \langle\langle 2\rangle\rangle &\equiv \left\langle\left\langle e^{in(\phi_1-\phi_2)}\right\rangle\right\rangle, \\ \langle\langle 4\rangle\rangle &\equiv \left\langle\left\langle e^{in(\phi_1+\phi_2-\phi_3-\phi_4)}\right\rangle\right\rangle, \\ \langle\langle 6\rangle\rangle &\equiv \left\langle\left\langle e^{in(\phi_1+\phi_2+\phi_3-\phi_4-\phi_5-\phi_6)}\right\rangle\right\rangle. \end{aligned} \tag{8}$$

Here ϕ_i $(i = 1, \ldots, 6)$ are the azimuthal angles of one unique combination of multiple particles in an event, n is the harmonic number, and $\langle\langle\cdots\rangle\rangle$ represents the average over all combinations from all events within a given multiplicity range. The corresponding cumulants, $c_n\{4\}$ and $c_n\{6\}$, are calculated as follows [54]:

$$\begin{aligned} c_n\{4\} &= \langle\langle 4\rangle\rangle - 2 \times \langle\langle 2\rangle\rangle^2, \\ c_n\{6\} &= \langle\langle 6\rangle\rangle - 9 \times \langle\langle 4\rangle\rangle\langle\langle 2\rangle\rangle + 12 \times \langle\langle 2\rangle\rangle^3. \end{aligned} \tag{9}$$

The Fourier harmonics v_n that characterize the global azimuthal behavior are related to the multi-particle cumulants [54] using

$$\begin{aligned} v_n\{4\} &= \sqrt[4]{-c_n\{4\}}, \\ v_n\{6\} &= \sqrt[6]{\frac{1}{4}c_n\{6\}}. \end{aligned} \tag{10}$$

Note that a non-imaginary $v_n\{4\}$ coefficient, which would suggest a bulk medium collective behavior, requires having a negative $c_n\{4\}$ value.

4.3. Systematic uncertainties

Systematic uncertainties in this analysis include those from the experimental procedure for obtaining the two-particle v_n harmonics, as well as from the jet subtraction procedure.

The experimental systematic effects are evaluated by varying conditions in extracting $v_2^{\rm sub}\{2\}$, $v_3^{\rm sub}\{2\}$, $v_2\{4\}$ and $v_2\{6\}$ values. The systematic uncertainties are found to have no significant dependence on $p_{\rm T}$ and $\sqrt{s}$ so they are quoted to be constant percentages over the entire $p_{\rm T}$ range for all collision energies. Experimental systematic uncertainties due to track quality requirements are

Table 2
Summary of systematic uncertainties for multiplicity-dependent $v_n^{\mathrm{sub}}\{2\}$ from two-particle correlations (after correcting for jet correlations), and $v_2\{4\}$, $v_2\{6\}$ from multi-particle correlations in pp collisions. Different multiplicity ranges are represented as $[m, n)$.

Source	$v_2^{\mathrm{sub}}\{2\}$ (%)			$v_3^{\mathrm{sub}}\{2\}$ (%)			$v_2\{4\}$, $v_2\{6\}$ (%)	
	$[0, 40)$	$[40, 85)$	$[85, \infty)$	$[0, 40)$	$[40, 85)$	$[85, \infty)$	$[0, 85)$	$[85, \infty)$
HLT trigger bias	–	–	2	–	–	2	–	2
Track quality cuts	1	1	1	1	1	1	1	1
Pileup effects	1.5	1.5	1.5	1.5	1.5	1.5	1.5	1.5
Vertex dependence	1.5	1.5	1.5	1.5	1.5	1.5	1.5	1.5
Jet subtraction	18	9.5	6.5	26.8	17	8.5	–	–
Total	18.2	9.8	7.2	27	17.3	8.8	2.4	3.1

examined by varying the track selection thresholds for $d_z/\sigma(d_z)$ and $d_{xy}/\sigma(d_{xy})$ from 2 to 5. A comparison of high-multiplicity pp data for a given multiplicity range but collected by two different HLT triggers with different trigger efficiencies is made to study potential trigger biases. The possible contamination of residual pileup events, especially for 5 and 7 TeV data, is also investigated by varying the pileup selection of events in performing the analysis, from no pileup rejection at all to selecting events with only one reconstructed vertex. The sensitivity of the results to the primary vertex position (z_{vtx}) is quantified by comparing results at different z_{vtx} locations over a 30 cm wide range.

In the jet subtraction procedure for $v_n\{2\}$ measurements, while the factor $Y_{\mathrm{jet}}/Y_{\mathrm{jet}}(10 \le N_{\mathrm{trk}}^{\mathrm{offline}} < 20)$ accounts for any bias in the magnitude of jet-like associated yield due to multiplicity selection, a change in the $\Delta\phi$ width of away side yields could lead to residual jet effects in $v_n\{2\}$ results. This systematic uncertainty is evaluated by integrating the associated yields in the $|\Delta\eta| > 2$ region over fixed $\Delta\phi$ windows of $|\Delta\phi| < \pi/3$ and $|\Delta\phi - \pi| < \pi/3$ on the near and away sides, respectively. When extracting v_n^{sub} results, the Y_{jet} parameter in Eq. (7) is then replaced by this difference of the near and away side yields. By taking the difference of the yields in two $\Delta\phi$ windows symmetric around $\Delta\phi = \pi/2$, contributions from the second and fourth Fourier components are cancelled. By choosing the $\Delta\phi$ window size to be $2\pi/3$, any contribution from the third Fourier component to the near and away side associated yields is also cancelled. Any dependence of this yield difference on the event multiplicity (beyond that induced by the $Y_{\mathrm{jet}}/Y_{\mathrm{jet}}(10 \le N_{\mathrm{trk}}^{\mathrm{offline}} < 20)$ factor) would indicate a modification of jet correlation width in $\Delta\phi$. The systematic uncertainty of v_n due to this effect is estimated to be 16%, 9%, and 6% for $N_{\mathrm{trk}}^{\mathrm{offline}} < 40$, $40 \le N_{\mathrm{trk}}^{\mathrm{offline}} < 85$, and $N_{\mathrm{trk}}^{\mathrm{offline}} > 85$, respectively. In the same sense, any multiplicity dependence of the $\Delta\eta$ distribution of the away side would indicate a modification of the jet correlation. The $\Delta\eta$ distribution is investigated in a fixed window $|\Delta\phi - \pi| < \pi/16$ for different $N_{\mathrm{trk}}^{\mathrm{offline}}$ ranges, resulting in systematic uncertainties of 8%, 3%, and 2.5% for $N_{\mathrm{trk}}^{\mathrm{offline}} < 40$, $40 \le N_{\mathrm{trk}}^{\mathrm{offline}} < 85$, and $N_{\mathrm{trk}}^{\mathrm{offline}} > 85$, respectively. In addition, by separating events in a given multiplicity range into two groups corresponding to the top and bottom 30% in the leading particle p_{T} distribution, jet correlations are either strongly enhanced or suppressed in a controlled manner. After applying the subtraction procedure, the v_n results for the two event groups are consistent within 5%.

Table 2 summarizes various sources of systematic uncertainties in this analysis for multiplicity-dependent results. The same sources apply to p_{T} differential results, leading to total experimental systematic uncertainty of 5% and uncertainties from the jet subtraction procedure of 9%, 13%, 23%, and 37% for $p_{\mathrm{T}}^{\mathrm{trig}} < 2.2\,\mathrm{GeV}/c$, $2.2 \le p_{\mathrm{T}}^{\mathrm{trig}} < 3.6\,\mathrm{GeV}/c$, $3.6 \le p_{\mathrm{T}}^{\mathrm{trig}} < 4.6\,\mathrm{GeV}/c$, and $p_{\mathrm{T}}^{\mathrm{trig}} \ge 4.6\,\mathrm{GeV}/c$, respectively.

Systematic uncertainties originating from different sources are added in quadrature to obtain the overall systematic uncertainty shown as boxes in the figures. No energy dependence has been observed for the systematic uncertainties, therefore, they are only shown for 13 TeV results. Because of insufficient statistical precision, the uncertainties in v_3 resulting from the experimental procedure are assumed to be the same as those in v_2, as was done in Refs. [39,43]. For the same reason, the systematic uncertainties on the $v_2\{2\}$ results for V^0 particles that result from the variation of selection criteria, alternative detector geometry and a MC closure test are obtained from studies performed for pPb collisions in Ref. [39], while those resulting from systematic bias of the HLT trigger and jet subtraction method are taken to be the same as for the inclusive charged particles. Different particle species have different η distributions, which can affect the comparison of results if there is a strong η dependence. This effect is found to be negligible by comparing $v_2\{2\}$ results for V^0 particles with different reconstruction efficiency corrections for the η distribution. The relative systematic uncertainties for the two-particle $V_{n\Delta}$ coefficients as a function of $N_{\mathrm{trk}}^{\mathrm{offline}}$ in Fig. 4 (described in Section 5.2) are exactly twice those for the corresponding v_n harmonics, since $V_{n\Delta} = v_n^2$ when trigger and associated particles are selected from the same p_{T} range. In the same way, relative systematic uncertainties for multi-particle $c_2\{m\}$ measurements as a function of $N_{\mathrm{trk}}^{\mathrm{offline}}$ in Fig. 9 (described in Section 5.3) are exactly m times those for the corresponding $v_2\{m\}$ harmonics, where $m = 4$ or 6.

5. Results

5.1. Two-particle correlation functions

Fig. 1 shows the 2D $\Delta\eta$–$\Delta\phi$ correlation functions, for pairs of a charged (top), a $\mathrm{K}_{\mathrm{S}}^0$ (middle), or a $\Lambda/\overline{\Lambda}$ (bottom) trigger particle with a charged associated particle, in low-multiplicity ($10 \le N_{\mathrm{trk}}^{\mathrm{offline}} < 20$, left) and high-multiplicity ($105 \le N_{\mathrm{trk}}^{\mathrm{offline}} < 150$, right) pp collisions at $\sqrt{s} = 13\,\mathrm{TeV}$. Both trigger and associated particles are selected from the p_{T} range of 1–3 GeV/c. For all three types of particles at high multiplicity, in addition to the correlation peak near $(\Delta\eta, \Delta\phi) = (0, 0)$ that results from jet fragmentation, a long-range ridge structure is seen at $\Delta\phi \approx 0$ extending at least 4 units in $|\Delta\eta|$, while such a structure is not observed in low multiplicity events. On the away side ($\Delta\phi \approx \pi$) of the correlation functions, a long-range structure is also seen and found to exhibit a much larger magnitude compared to that on the near side for this p_{T} range. This away side correlation structure contains contributions from back-to-back jets, which need to be accounted for before extracting any other source of correlations.

To investigate the observed correlations in finer detail, the 2D distributions shown in Fig. 1 are reduced to one-dimensional (1D) distributions in $\Delta\phi$ by averaging over $|\Delta\eta| < 1$ (defined as the "short-range region") and $|\Delta\eta| > 2$ (defined as the "long-range region"), respectively, as done in Refs. [1,4,13,14]. Fig. 2 shows exam-

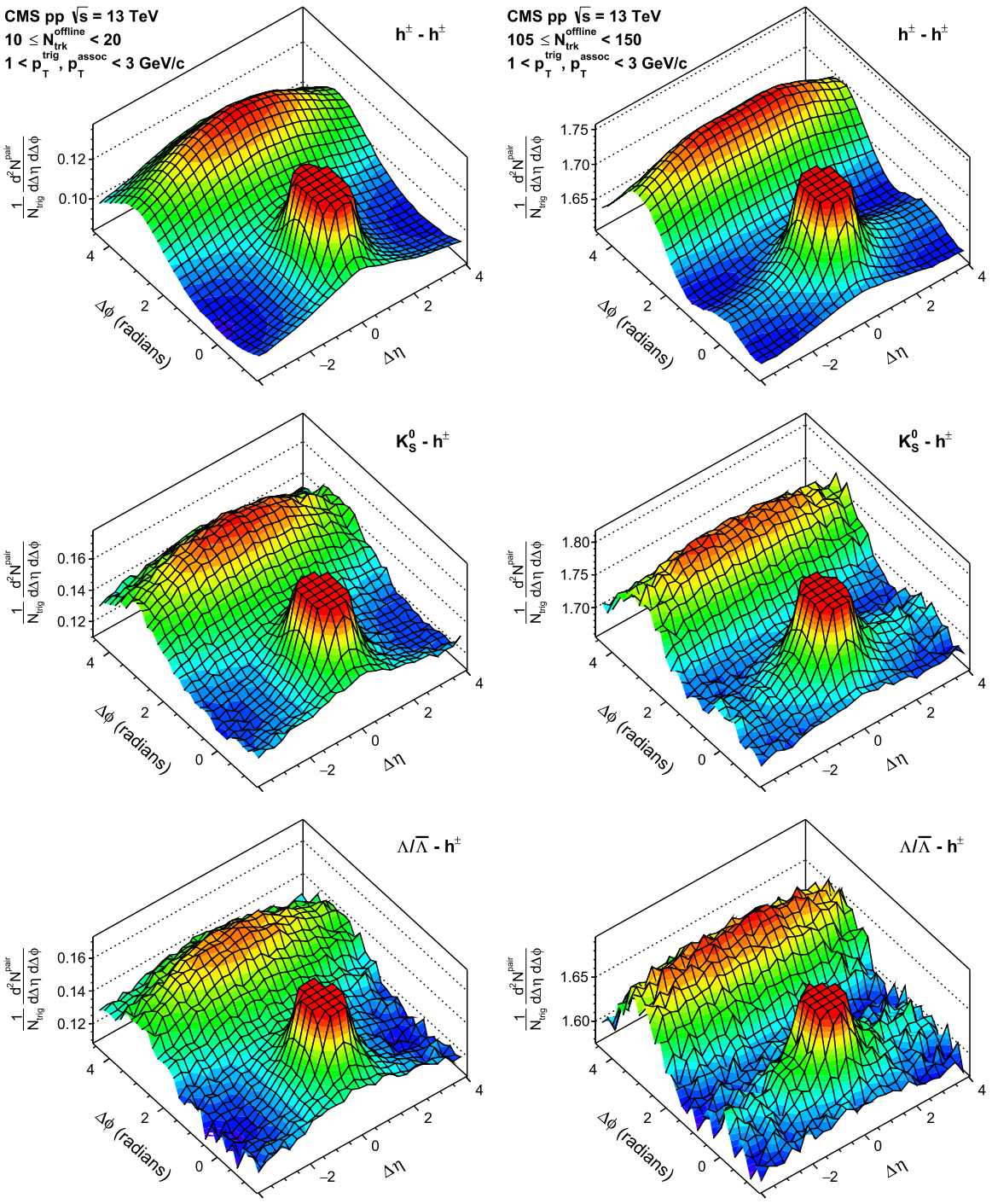

Fig. 1. The 2D two-particle correlation functions for inclusive charged particles (top), K^0_S particles (middle), and $\Lambda/\overline{\Lambda}$ particles (bottom), with $1 < p_T^{trig} < 3\,GeV/c$ and associated charged particles with $1 < p_T^{assoc} < 3\,GeV/c$, in low-multiplicity ($10 \le N_{trk}^{offline} < 20$, left) and high-multiplicity ($105 \le N_{trk}^{offline} < 150$, right) pp collisions at $\sqrt{s} = 13\,TeV$.

ples of 1D $\Delta\phi$ correlation functions for trigger particles composed of inclusive charged particles (left), K^0_S particles (middle), and $\Lambda/\overline{\Lambda}$ particles (right), in the multiplicity range $10 \le N_{trk}^{offline} < 20$ (open symbols) and $105 \le N_{trk}^{offline} < 150$ (filled symbols). The curves show the Fourier fits from Eq. (4) to the long-range region, which will be discussed in detail in Section 5.2. To represent the correlated portion of the associated yield, each distribution is shifted to have zero associated yield at its minimum following the standard zero-yield-at-minimum (ZYAM) procedure [43]. An enhanced correlation at $\Delta\phi \approx 0$ in the long-range region is observed for $105 \le N_{trk}^{offline} < 150$, while such a structure is not presented for $10 \le N_{trk}^{offline} < 20$. As illustrated in Fig. 1 (right), the near side long-range ridge structure remains nearly constant in $\Delta\eta$. Therefore, the near side jet correlation can be extracted by taking a difference of 1D $\Delta\phi$ projections between the short- and long-range regions, as shown in the bottom panels in Fig. 2.

After subtracting the results, with the ZYAM procedure applied, for low-multiplicity $10 \le N_{trk}^{offline} < 20$ scaled by $Y_{jet}/Y_{jet}(10 \le N_{trk}^{offline} < 20)$ as in Eq. (7), the long-range 1D $\Delta\phi$ correlation functions in the high-multiplicity range $105 \le N_{trk}^{offline} < 150$ for pp

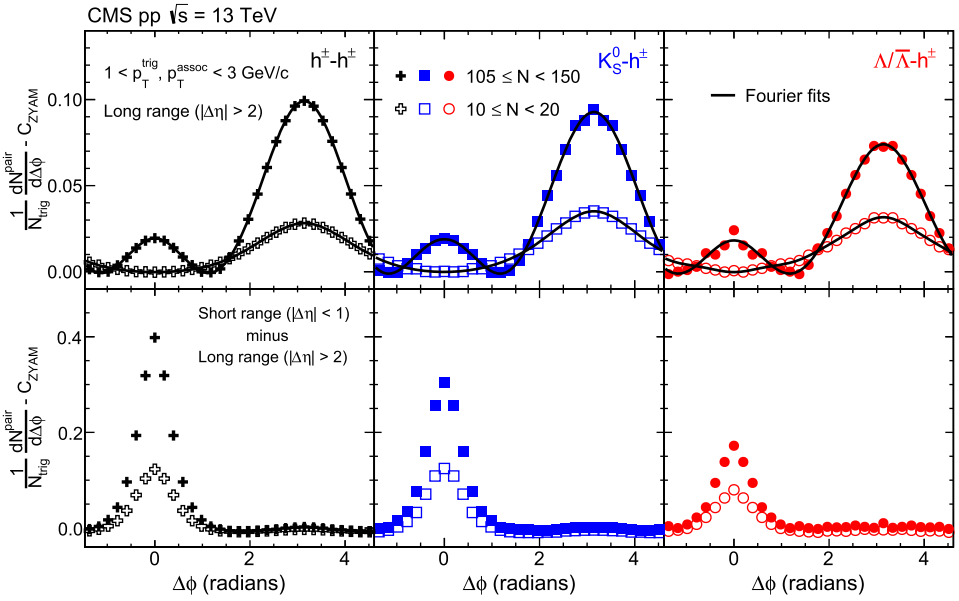

Fig. 2. The 1D $\Delta\phi$ correlation functions for the long-range (top) and short- minus long-range (bottom) regions after applying the ZYAM procedure in the multiplicity range $10 \leq N_{\mathrm{trk}}^{\mathrm{offline}} < 20$ (open symbols) and $105 \leq N_{\mathrm{trk}}^{\mathrm{offline}} < 150$ (filled symbols) of pp collisions at $\sqrt{s} = 13\,\mathrm{TeV}$, for trigger particles composed of inclusive charged particles (left, crosses), $\mathrm{K}^0_{\mathrm{S}}$ particles (middle, squares), and $\Lambda/\overline{\Lambda}$ particles (right, circles). A selection of 1–3 GeV/c for both $p_{\mathrm{T}}^{\mathrm{trig}}$ and $p_{\mathrm{T}}^{\mathrm{assoc}}$ is used in all cases.

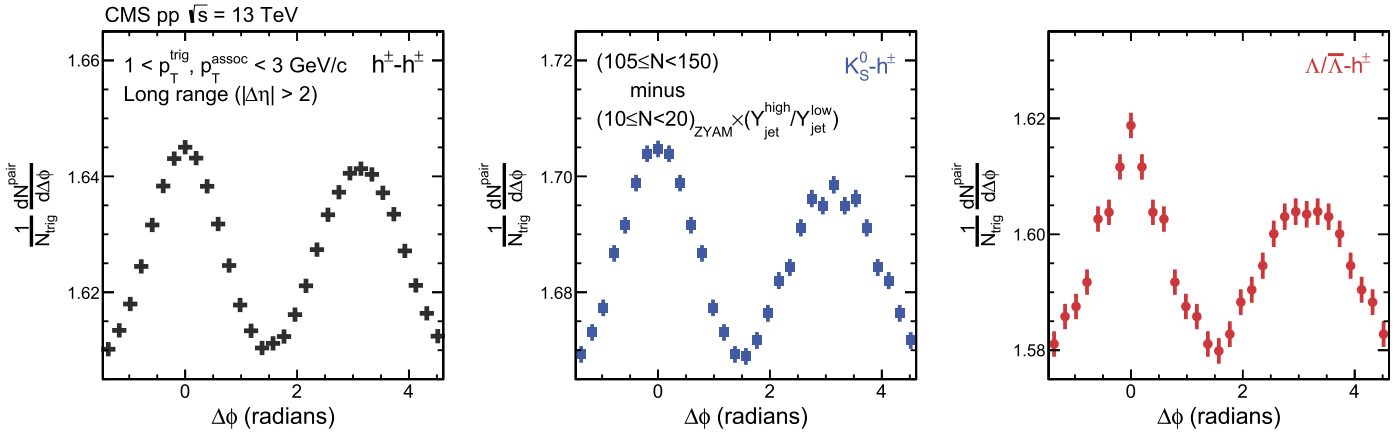

Fig. 3. The 1D $\Delta\phi$ correlation functions for the long-range regions in the multiplicity range $105 \leq N_{\mathrm{trk}}^{\mathrm{offline}} < 150$ of pp collisions at $\sqrt{s} = 13\,\mathrm{TeV}$, after subtracting scaled results from $10 \leq N_{\mathrm{trk}}^{\mathrm{offline}} < 20$ with the ZYAM procedure applied. A selection of 1–3 GeV/c for both $p_{\mathrm{T}}^{\mathrm{trig}}$ and $p_{\mathrm{T}}^{\mathrm{assoc}}$ is used in all cases.

collisions at $\sqrt{s} = 13\,\mathrm{TeV}$ are shown in Fig. 3, for trigger particles composed of inclusive charged particles (left), $\mathrm{K}^0_{\mathrm{S}}$ (middle), and $\Lambda/\overline{\Lambda}$ (right) particles. A "double-ridge" structure on the near and away side is observed after subtraction of jet correlations. The shape of this structure, which is dominated by a second-order Fourier component, is similar to what has been observed in pPb [4–7] and PbPb [13,14,16,17,55] collisions.

5.2. Two-particle Fourier harmonics v_n

Fourier coefficients, $V_{n\Delta}$, extracted from 1D $\Delta\phi$ two-particle correlation functions for the long-range $\Delta\eta$ region using Eq. (4), are first studied for inclusive charged hadrons. Fig. 4 shows the $V_{2\Delta}$ and $V_{3\Delta}$ values for pairs of inclusive charged particles averaged over $0.3 < p_{\mathrm{T}} < 3.0\,\mathrm{GeV}/c$ as a function of multiplicity in pp collisions at $\sqrt{s} = 13\,\mathrm{TeV}$, before and after correcting for back-to-back jet correlations estimated from low-multiplicity data ($10 \leq N_{\mathrm{trk}}^{\mathrm{offline}} < 20$). The $V_{n\Delta}$ results for 5 and 7 TeV are equal to the 13 TeV results within the uncertainties.

Before corrections, the $V_{2\Delta}$ coefficients are found to remain relatively constant as a function of multiplicity. This behavior is very different from the PYTHIA 8 tune CUETP8M1 MC simulation, where the only source of long-range correlations is back-to-back jets and the $V_{2\Delta}$ coefficients decrease with $N_{\mathrm{trk}}^{\mathrm{offline}}$. The $V_{3\Delta}$ coefficients found using the PYTHIA 8 simulation are always negative because of dominant contributions at $\Delta\phi \approx \pi$ from back-to-back jets [55], with their magnitudes decreasing as a function of $N_{\mathrm{trk}}^{\mathrm{offline}}$. A similar trend is seen in the data for the low multiplicity region, $N_{\mathrm{trk}}^{\mathrm{offline}} < 90$. However, for $N_{\mathrm{trk}}^{\mathrm{offline}} \geq 90$, the $V_{3\Delta}$ coefficients in pp data change to positive values. This transition directly indicates a new phenomena that is not present in the PYTHIA 8 simulation. After applying the jet correction procedure detailed in Section 4.1, $V_{2\Delta}$ exhibits an increase with multiplicity for $N_{\mathrm{trk}}^{\mathrm{offline}} \lesssim 100$, and reaches a relatively constant value for the higher $N_{\mathrm{trk}}^{\mathrm{offline}}$ region. The $V_{3\Delta}$ values after subtraction of jet correlations become positive over the entire multiplicity range and increase with multiplicity.

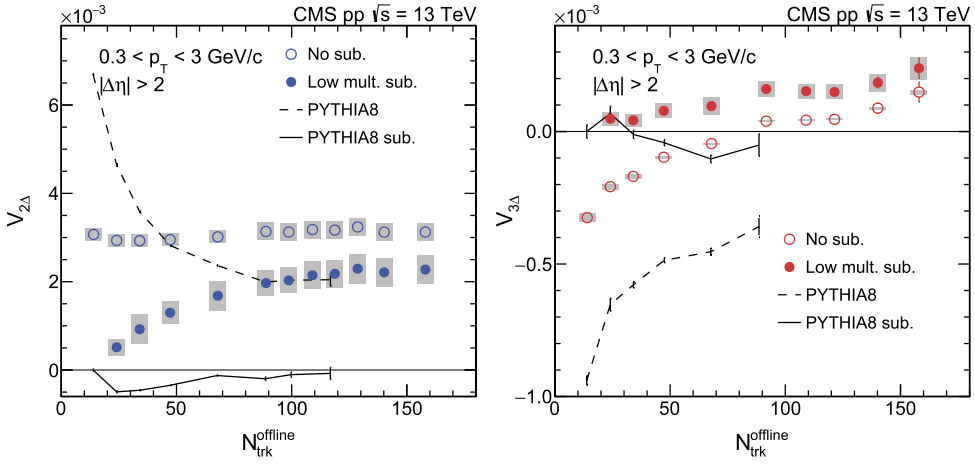

Fig. 4. The second-order (left) and third-order (right) Fourier coefficients, $V_{2\Delta}$ and $V_{3\Delta}$, of long-range ($|\Delta\eta| > 2$) two-particle $\Delta\phi$ correlations as a function of $N_{\mathrm{trk}}^{\mathrm{offline}}$ for charged particles, averaged over $0.3 < p_{\mathrm{T}} < 3.0\,\mathrm{GeV}/c$, in pp collisions at $\sqrt{s} = 13\,\mathrm{TeV}$, before (open) and after (filled) correcting for back-to-back jet correlations, estimated from the $10 \leq N_{\mathrm{trk}}^{\mathrm{offline}} < 20$ range. Results from PYTHIA 8 tune CUETP8M1 simulation are shown as curves. The error bars correspond to statistical uncertainties, while the shaded areas denote the systematic uncertainties.

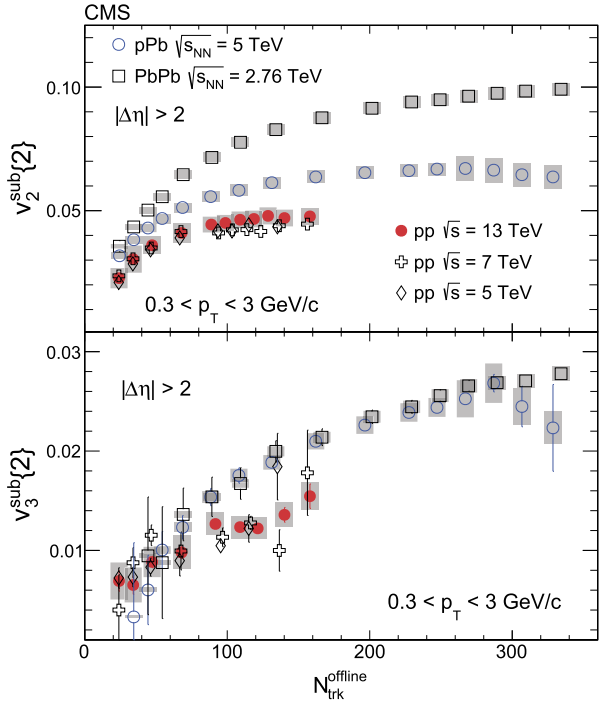

Fig. 5. The v_2^{sub} (top) and v_3^{sub} (bottom) results of charged particles as a function of $N_{\mathrm{trk}}^{\mathrm{offline}}$, averaged over $0.3 < p_{\mathrm{T}} < 3.0\,\mathrm{GeV}/c$, in pp collisions at $\sqrt{s} = 5$, 7, and 13 TeV, pPb collisions at $\sqrt{s_{\mathrm{NN}}} = 5\,\mathrm{TeV}$, and PbPb collisions $\sqrt{s_{\mathrm{NN}}} = 2.76\,\mathrm{TeV}$, after correcting for back-to-back jet correlations estimated from low-multiplicity data. The error bars correspond to the statistical uncertainties, while the shaded areas denote the systematic uncertainties. Systematic uncertainties are found to have no dependence on $\sqrt{s}$ for pp results and therefore are only shown for 13 TeV.

The elliptic (v_2) and triangular (v_3) flow harmonics for charged particles with $0.3 < p_{\mathrm{T}} < 3.0\,\mathrm{GeV}/c$, after applying the jet correction procedure, are then extracted from the two-particle Fourier coefficients obtained using Eq. (5), and are shown in Fig. 5 for pp collisions at $\sqrt{s} = 5$, 7, and 13 TeV. The previously published pPb data at $\sqrt{s_{\mathrm{NN}}} = 5\,\mathrm{TeV}$ and PbPb data at $\sqrt{s_{\mathrm{NN}}} = 2.76\,\mathrm{TeV}$ [43] are also shown for comparison among different collision systems.

Within experimental uncertainties, for pp collisions at all three energies, there is no or only a very weak energy dependence for the v_2^{sub} values. The v_2^{sub} results for pp collisions show a similar pattern as the pPb results, becoming relatively constant as $N_{\mathrm{trk}}^{\mathrm{offline}}$ increases, while the PbPb results show a moderate increase over the entire $N_{\mathrm{trk}}^{\mathrm{offline}}$ range shown in Fig. 5. Overall, the pp data show a smaller v_2^{sub} signal than pPb data over a wide multiplicity range, and both systems show smaller v_2^{sub} values than for the PbPb system.

The v_3^{sub} values of the pp data are comparable to those observed in pPb and PbPb collisions in the very low multiplicity region $N_{\mathrm{trk}}^{\mathrm{offline}} < 60$, although systematic uncertainties are large for all the three systems. At higher $N_{\mathrm{trk}}^{\mathrm{offline}}$, v_3^{sub} in pp collisions increases with multiplicity, although at a slower rate than observed in pPb and PbPb collisions.

The v_2 values reported by the ATLAS Collaboration for pp collisions at $\sqrt{s} = 13\,\mathrm{TeV}$ in Ref. [2] have a different multiplicity dependence than the results presented in this paper. A nearly constant v_2 value is observed over the entire multiplicity range. This distinct difference, especially in the low multiplicity region, is rooted in the different approaches employed in identifying the v_2 signal from jet-like correlations. In the method from CMS and also previous ATLAS and ALICE analyses [5,6,56], v_2 is always extracted with respect to all of the particles in each event. As seen in Eq. (4), the Fourier coefficients in the current analysis represent an oscillation multiplied by the full N_{assoc}. In the new approach by the ATLAS Collaboration [2], v_2 is extracted with respect to a subset of particles in each event. In Ref. [2], their equivalent of our Eq. (4) uses a smaller number than the full N_{assoc} in the events, thereby assuming that some of the particles do not participate in the underlying processes producing the observed azimuthal correlations. As a result, using the method of Ref. [2], a $\cos(2\Delta\phi)$ modulation with exactly the same amplitude would yield a bigger $V_{n\Delta}$ parameter compared to that found using Eq. (4). This, in turn, leads to larger v_2 values comparing to results obtained with respect to all of the particles. The difference between the two methods becomes larger as $N_{\mathrm{trk}}^{\mathrm{offline}}$ decreases. It was checked that when applying exactly the same kinematic selections and analysis methods, no discrepancy is found between the two experiments. In the study of v_2 from multiparticle correlations, as will be discussed in Section 5.3, the v_2 is always considered with respect to all the particles in the event for each multiplicity class, which is consistent with the method used in this paper to extract v_2 from two-particle correlations.

The v_2 results as a function of p_{T} for high-multiplicity pp events at $\sqrt{s} = 5$, 7, and 13 TeV are shown in Fig. 6 before (top) and after (bottom) correcting for jet correlations. To compare re-

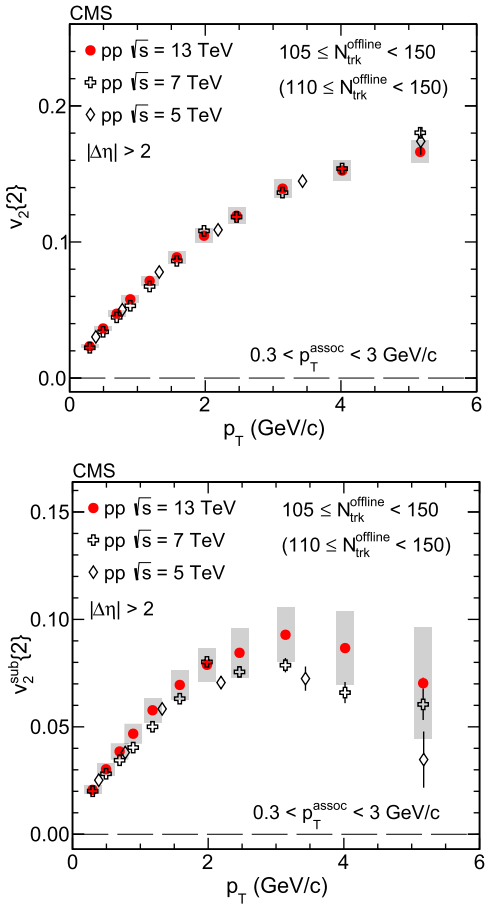

Fig. 6. The v_2 results of inclusive charged particles, before (top) and after (bottom) subtracting correlations from low-multiplicity events, as a function of p_T in pp collisions at $\sqrt{s} = 13$ TeV for $105 \leq N_{trk}^{offline} < 150$ and at $\sqrt{s} = 5, 7$ TeV for $110 \leq N_{trk}^{offline} < 150$. The error bars correspond to the statistical uncertainties, while the shaded areas denote the systematic uncertainties. Systematic uncertainties are found to have no dependence on $\sqrt{s}$ for pp results and therefore are only shown for 13 TeV.

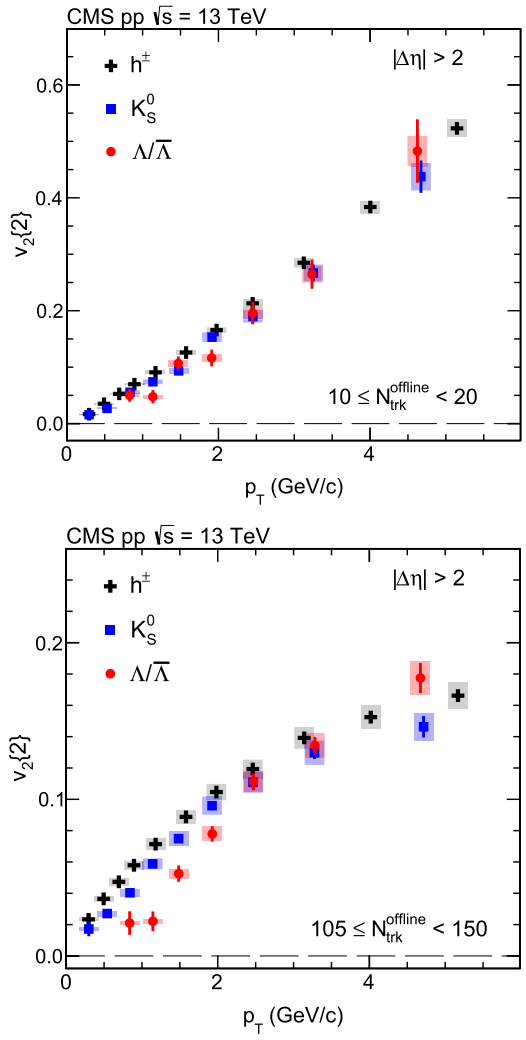

Fig. 7. The v_2 results for inclusive charged particles, K_S^0 and $\Lambda/\overline{\Lambda}$ particles as a function of p_T in pp collisions at $\sqrt{s} = 13$ TeV, for $10 \leq N_{trk}^{offline} < 20$ (top) and $105 \leq N_{trk}^{offline} < 150$ (bottom). The error bars correspond to the statistical uncertainties, while the shaded areas denote the systematic uncertainties.

sults with similar average $N_{trk}^{offline}$, $105 \leq N_{trk}^{offline} < 150$ is chosen for 13 TeV while $110 \leq N_{trk}^{offline} < 150$ is chosen for 5 and 7 TeV. Little energy dependence is observed for the p_T-differential v_2 results, especially before correcting for jet correlations, as shown in Fig. 6 (top). This conclusion also holds after jet correction procedure for v_2^{sub} results (Fig. 6, bottom) within systematic uncertainties, although systematic uncertainties for v_2^{sub} are significantly higher at high p_T because of the large magnitude of the subtracted term. This observation is consistent with the energy independence of associated long-range yields on the near side reported in Ref. [3]. The observed p_T dependence of v_2^{sub}, in high-multiplicity pp events with peak values at 2–3 GeV/c at various energies, is similar to that in pPb [38,43,56] and PbPb [14,57,58] collisions.

The dependence of the elliptic flow harmonic on particle species can shed further light on the nature of the correlations. The v_2 data as a function of p_T for identified K_S^0 and $\Lambda/\overline{\Lambda}$ particles are extracted for pp collisions at $\sqrt{s} = 13$ TeV. Fig. 7 shows the results for a low ($10 \leq N_{trk}^{offline} < 20$) and a high ($105 \leq N_{trk}^{offline} < 150$) multiplicity range before applying the jet correction procedure.

At low multiplicity (Fig. 7 top), the v_2 values are found to be similar for charged particles, K_S^0 and $\Lambda/\overline{\Lambda}$ hadrons across most of the p_T range within statistical uncertainties, similar to the observation in pPb collisions at $\sqrt{s_{NN}} = 5$ TeV [39]. This would be consistent with the expectation that back-to-back jets are the dominant source of long-range correlations on the away side in low-multiplicity pp events. Moving to high-multiplicity pp events ($105 \leq N_{trk}^{offline} < 150$, Fig. 7 bottom), a clear deviation of v_2 among various particle species is observed. In the lower p_T region of $\lesssim 2.5$ GeV/c, the v_2 value of K_S^0 is greater than that of $\Lambda/\overline{\Lambda}$ at a given p_T value. Both are consistently below the inclusive charged particle v_2 values. Since most charged particles are pions in this p_T range, this indicates that lighter particle species exhibit a stronger azimuthal anisotropy signal. A similar trend was first observed in AA collisions at RHIC [59,60], and later also seen in pPb collisions at the LHC [38,39]. This behavior is found to be qualitatively consistent with both hydrodynamic models [44,45] and an alternative initial state interpretation [47]. At $p_T > 2.5$ GeV/c, the v_2 values of $\Lambda/\overline{\Lambda}$ particles tend to become greater than those of K_S^0 particles. This reversed ordering of K_S^0 and $\Lambda/\overline{\Lambda}$ at high p_T is similar to what was previously observed in pPb and PbPb collisions [39].

After applying the correction for jet correlations, the v_2^{sub} results as a function of p_T for $105 \leq N_{trk}^{offline} < 150$ are shown in Fig. 8 (top) for the identified particles and charged hadrons. The v_2^{sub} values for all three types of particles are found to increase with p_T, reaching 0.08–0.10 at $2 < p_T < 3$ GeV/c, and then show a trend of decreasing v_2^{sub} values for higher p_T values. The par-

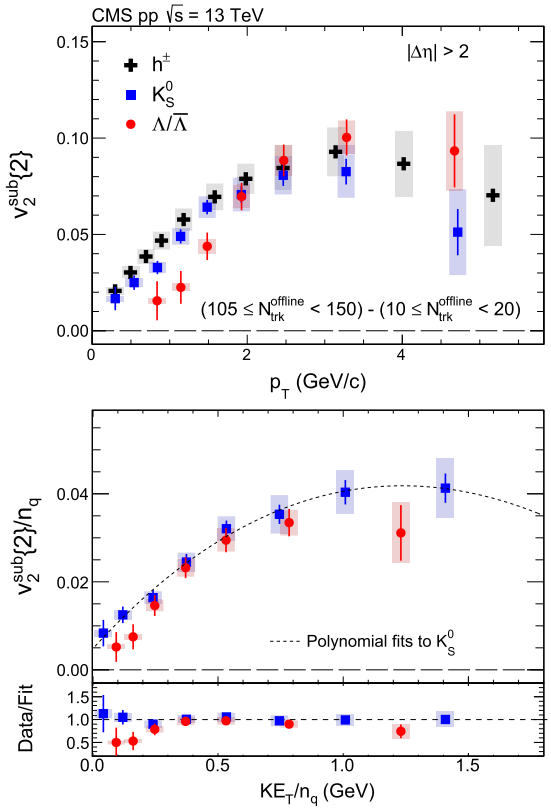

Fig. 8. Top: the v_2^{sub} results of inclusive charged particles, $\mathrm{K}^0_{\mathrm{S}}$ and $\Lambda/\overline{\Lambda}$ particles as a function of p_{T} for $105 \leq N_{\mathrm{trk}}^{\mathrm{offline}} < 150$, after correcting for back-to-back jet correlations estimated from low-multiplicity data. Bottom: the n_{q}-scaled v_2^{sub} results for $\mathrm{K}^0_{\mathrm{S}}$ and $\Lambda/\overline{\Lambda}$ particles as a function of $KE_{\mathrm{T}}/n_{\mathrm{q}}$. Ratios of $v_2^{\mathrm{sub}}/n_{\mathrm{q}}$ for $\mathrm{K}^0_{\mathrm{S}}$ and $\Lambda/\overline{\Lambda}$ particles to a smooth fit function of data for $\mathrm{K}^0_{\mathrm{S}}$ particles are also shown. The error bars correspond to the statistical uncertainties, while the shaded areas denote the systematic uncertainties.

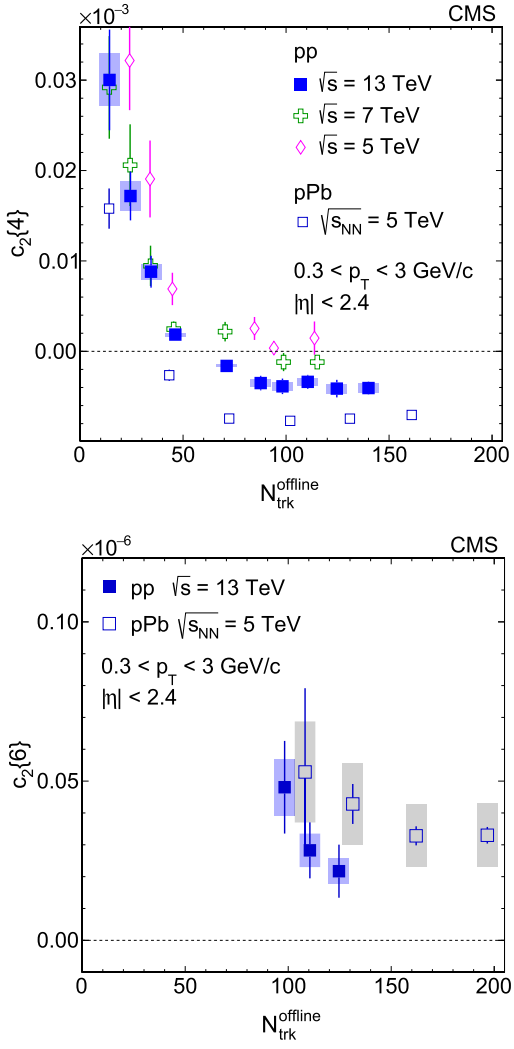

Fig. 9. The $c_2\{4\}$ (top) and $c_2\{6\}$ (bottom) values as a function of $N_{\mathrm{trk}}^{\mathrm{offline}}$ for charged particles, averaged over $0.3 < p_{\mathrm{T}} < 3.0\,\mathrm{GeV}/c$ and $|\eta| < 2.4$, in pp collisions at $\sqrt{s} = 5$, 7, and 13 TeV. The pPb data at $\sqrt{s_{\mathrm{NN}}} = 5\,\mathrm{TeV}$ are also plotted for comparison. The error bars correspond to the statistical uncertainties, while the shaded areas denote the systematic uncertainties. Systematic uncertainties are found to have no dependence on $\sqrt{s}$ for pp results and therefore are only shown for 13 TeV.

ticle mass ordering of v_2 values in the lower p_{T} region is also observed after applying jet correction procedure, while at higher p_{T} the ordering tends to reverse. As done in Ref. [39], the scaling behavior of v_2^{sub} divided by the number of constituent quarks, n_{q}, as a function of transverse kinetic energy per quark, $KE_{\mathrm{T}}/n_{\mathrm{q}}$, is investigated for high-multiplicity pp events in Fig. 8 (bottom). The dashed curve corresponds to a polynomial fit to the $\mathrm{K}^0_{\mathrm{S}}$ data. The ratio of n_{q}-scaled v_2^{sub} results for $\mathrm{K}^0_{\mathrm{S}}$ and $\Lambda/\overline{\Lambda}$ particles divided by this polynomial function fit is also shown in Fig. 8 (bottom). An approximate scaling is seen for $KE_{\mathrm{T}}/n_{\mathrm{q}} \gtrsim 0.2\,\mathrm{GeV}$ within about $\pm 10\%$.

5.3. Multi-particle correlations and collectivity

To further reduce the residual jet correlations on the away side and explore the possible collective nature of the long-range correlations, a four- and six-particle cumulant analysis is used to extract the elliptic flow harmonics, $v_2\{4\}$ and $v_2\{6\}$. The four-particle cumulant $c_2\{4\}$ values for charged particles with $0.3 < p_{\mathrm{T}} < 3.0\,\mathrm{GeV}/c$ are shown in Fig. 9 (top), as a function of $N_{\mathrm{trk}}^{\mathrm{offline}}$ for pp collisions at $\sqrt{s} = 5$, 7, and 13 TeV. The pPb data at $\sqrt{s_{\mathrm{NN}}} = 5\,\mathrm{TeV}$ [43] are also plotted for comparison. The six-particle cumulant $c_2\{6\}$ values for pp collisions at $\sqrt{s} = 13\,\mathrm{TeV}$ are shown in Fig. 9 (bottom), compared with pPb data at $\sqrt{s_{\mathrm{NN}}} = 5\,\mathrm{TeV}$ [43]. Due to statistical limitations, $c_2\{6\}$ values are only derived for high multiplicities (i.e., $N_{\mathrm{trk}}^{\mathrm{offline}} \approx 100$) for 13 TeV pp data.

The $c_2\{4\}$ values for pp data at all energies show a decreasing trend with increasing multiplicity, similar to that found for pPb collisions. An indication of energy dependence of $c_2\{4\}$ values is seen in Fig. 9 (top), where $c_2\{4\}$ tends to be larger for a given $N_{\mathrm{trk}}^{\mathrm{offline}}$ range at lower $\sqrt{s}$ energies. As average p_{T} values are slightly smaller at lower collision energies, the observed energy dependence may be related to smaller negative contribution to $c_2\{4\}$ from smaller p_{T}-averaged $v_2\{4\}$ signals. In addition, when selecting from a fixed multiplicity range, a larger positive contribution to $c_2\{4\}$ from larger jet-like correlations in the much rarer high-multiplicity events in lower energy pp collisions can also result in an energy dependence. At $N_{\mathrm{trk}}^{\mathrm{offline}} \approx 60$ for 13 TeV pp data, the $c_2\{4\}$ values become and remain negative as the multiplicity increases further. This behavior is similar to that observed for pPb data where the sign change occurs at $N_{\mathrm{trk}}^{\mathrm{offline}} \approx 40$, indicating a collective $v_2\{4\}$ signal [61]. For pp data at $\sqrt{s} = 5$ and 7 TeV, no significant negative values of $c_2\{4\}$ are observed within statistical uncertainties. The $c_2\{6\}$ values for pp data at 13 TeV show an increasing trend with decreasing multiplicity, similar to that found for pPb collisions. This trend might be due to a larger contribution to $c_2\{6\}$ from jet-like correlations in lower-multiplicity events.

To obtain $v_2\{4\}$ and $v_2\{6\}$ results using Eq. (10), the cumulants are required to be at least two standard deviations away from their

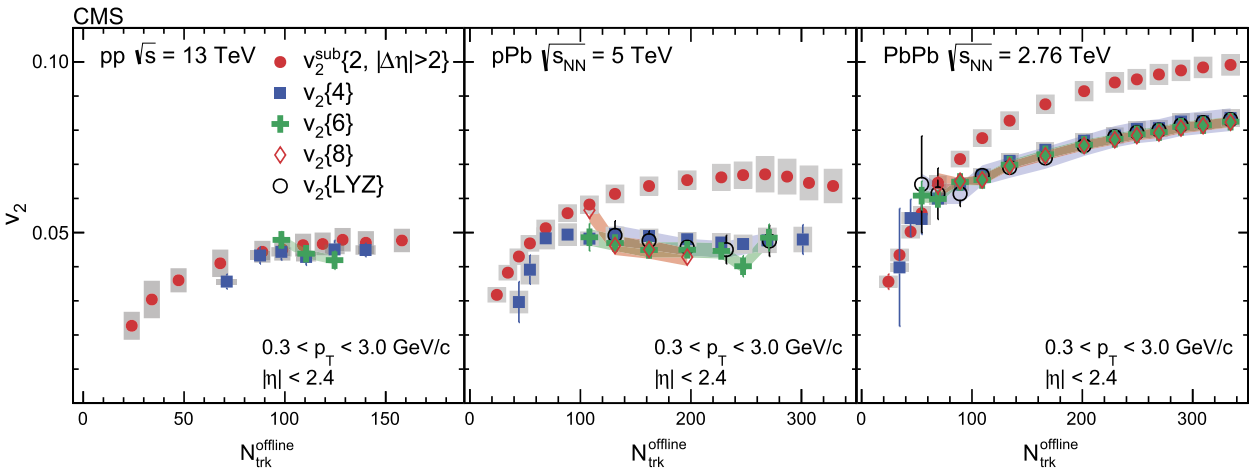

Fig. 10. Left: the $v_2^{\rm sub}\{2,|\Delta\eta|>2\}$, $v_2\{4\}$ and $v_2\{6\}$ values as a function of $N_{\rm trk}^{\rm offline}$ for charged particles, averaged over $0.3<p_{\rm T}<3.0\,{\rm GeV}/c$ and $|\eta|<2.4$, in pp collisions at $\sqrt{s}=13\,{\rm TeV}$. Middle: the $v_2^{\rm sub}\{2,|\Delta\eta|>2\}$, $v_2\{4\}$, $v_2\{6\}$, $v_2\{8\}$, and $v_2\{{\rm LYZ}\}$ values in pPb collisions at $\sqrt{s_{\rm NN}}=5\,{\rm TeV}$ [43]. Right: the $v_2^{\rm sub}\{2,|\Delta\eta|>2\}$, $v_2\{4\}$, $v_2\{6\}$, $v_2\{8\}$, and $v_2\{{\rm LYZ}\}$ values in PbPb collisions at $\sqrt{s_{\rm NN}}=2.76\,{\rm TeV}$ [43]. The error bars correspond to the statistical uncertainties, while the shaded areas denote the systematic uncertainties.

physics boundaries (i.e. $c_2\{4\}/\sigma_{c_2\{4\}}<-2$ and $c_2\{6\}/\sigma_{c_2\{6\}}>2$), so that the statistical uncertainties can be propagated as Gaussian fluctuations [62]. The $v_2\{4\}$ and $v_2\{6\}$ results, averaged over $0.3<p_{\rm T}<3.0\,{\rm GeV}/c$ and $|\eta|<2.4$, for pp collisions at $\sqrt{s}=13\,{\rm TeV}$ are shown in the left panel of Fig. 10, as a function of event multiplicity. The v_2 data obtained from long-range two-particle correlations after correcting for jet correlations ($v_2^{\rm sub}\{2,|\Delta\eta|>2\}$) are also shown for comparison.

Within experimental uncertainties, the multi-particle cumulant $v_2\{4\}$ and $v_2\{6\}$ values in high-multiplicity pp collisions are consistent with each other, similar to what was observed previously in pPb and PbPb collisions [40]. This provides strong evidence for the collective nature of the long-range correlations observed in pp collisions. However, unlike for pPb and PbPb collisions where $v_2^{\rm sub}\{2,|\Delta\eta|>2\}$ values show a larger magnitude than multi-particle cumulant v_2 results, the v_2 values obtained from two-, four-, and six-particle correlations are comparable in pp collisions at $\sqrt{s}=13\,{\rm TeV}$ within uncertainties. In the context of hydrodynamic models, the relative ratios of v_2 among two- and various orders of multi-particle correlations provide insights to the details of initial-state geometry fluctuations in pp and pPb systems. As shown in Ref. [46], the ratio of $v_2\{4\}$ to $v_2^{\rm sub}\{2,|\Delta\eta|>2\}$ is related to the total number of fluctuating sources in the initial stage of a collision. The comparable magnitudes of $v_2^{\rm sub}\{2,|\Delta\eta|>2\}$ and $v_2\{4\}$ signals observed in pp collisions, compared to pPb collisions at similar multiplicities, may indicate a smaller number of initial fluctuating sources that drive the long-range correlations seen in the final state. Meanwhile, it remains to be seen whether other proposed mechanisms [32–34] in interpreting the long-range correlations in pPb and PbPb collisions can also describe the features of multi-particle correlations seen in pp collisions.

6. Summary

The CMS detector has been used to measure two- and multi-particle azimuthal correlations with K^0_S, $\Lambda/\overline{\Lambda}$ and inclusive charged particles over a broad pseudorapidity and transverse momentum range in pp collisions at $\sqrt{s}=5$, 7, and 13 TeV. With the implementation of high-multiplicity triggers during the LHC 2010 and 2015 pp runs, the correlation data are explored over a broad particle multiplicity range. The observed long-range ($|\Delta\eta|>2$) correlations are quantified in terms of azimuthal anisotropy Fourier harmonics (v_n). The elliptic (v_2) and triangular (v_3) flow Fourier harmonics are extracted from long-range two-particle correlations. After subtracting contributions from back-to-back jet correlations estimated using low-multiplicity data, the v_2 and v_3 values are found to increase with multiplicity for $N_{\rm trk}^{\rm offline}\lesssim 100$, and reach a relatively constant value at higher values of $N_{\rm trk}^{\rm offline}$. The $p_{\rm T}$ dependence of the v_2 harmonics in high-multiplicity pp events is found to have no or very weak dependence on the collision energy. In low-multiplicity events, similar v_2 values as a function of $p_{\rm T}$ are observed for inclusive charged particles, K^0_S and $\Lambda/\overline{\Lambda}$, possibly reflecting a common back-to-back jet origin of the correlations for all particle species. Moving to the higher-multiplicity region, a particle species dependence of v_2 is observed with and without correcting for jet correlations. For $p_{\rm T}\lesssim 2\,{\rm GeV}/c$, the v_2 of K^0_S is found to be larger than that of $\Lambda/\overline{\Lambda}$. This behavior is similar to what was previously observed for identified particles produced in pPb and AA collisions at RHIC and the LHC. This mass ordering tends to reverse at higher $p_{\rm T}$ values. Finally, v_2 signals based on four- and six-particle correlations are observed for the first time in pp collisions. The v_2 values obtained with two-, four-, and six-particle correlations at $\sqrt{s}=13\,{\rm TeV}$ are found to be comparable within uncertainties. These observations provide strong evidence supporting the interpretation of a collective origin for the observed long-range correlations in high-multiplicity pp collisions.

Acknowledgements

We congratulate our colleagues in the CERN accelerator departments for the excellent performance of the LHC and thank the technical and administrative staffs at CERN and at other CMS institutes for their contributions to the success of the CMS effort. In addition, we gratefully acknowledge the computing centers and personnel of the Worldwide LHC Computing Grid for delivering so effectively the computing infrastructure essential to our analyses. Finally, we acknowledge the enduring support for the construction and operation of the LHC and the CMS detector provided by the following funding agencies: BMWFW and FWF (Austria); FNRS and FWO (Belgium); CNPq, CAPES, FAPERJ, and FAPESP (Brazil); MES (Bulgaria); CERN; CAS, MOST, and NSFC (China); COLCIENCIAS (Colombia); MSES and CSF (Croatia); RPF (Cyprus); SENESCYT (Ecuador); MoER, ERC IUT and ERDF (Estonia); Academy of Finland, MEC, and HIP (Finland); CEA and CNRS/IN2P3 (France); BMBF, DFG, and HGF (Germany); GSRT (Greece); OTKA and NIH (Hungary); DAE and DST (India); IPM (Iran); SFI (Ireland); INFN (Italy);

MSIP and NRF (Republic of Korea); LAS (Lithuania); MOE and UM (Malaysia); BUAP, CINVESTAV, CONACYT, LNS, SEP, and UASLP-FAI (Mexico); MBIE (New Zealand); PAEC (Pakistan); MSHE and NSC (Poland); FCT (Portugal); JINR (Dubna); MON, RosAtom, RAS and RFBR (Russia); MESTD (Serbia); SEIDI and CPAN (Spain); Swiss Funding Agencies (Switzerland); MST (Taipei); ThEPCenter, IPST, STAR and NSTDA (Thailand); TUBITAK and TAEK (Turkey); NASU and SFFR (Ukraine); STFC (United Kingdom); DOE and NSF (USA).

Individuals have received support from the Marie-Curie program and the European Research Council and EPLANET (European Union); the Leventis Foundation; the Alfred P. Sloan Foundation; the Alexander von Humboldt Foundation; the Belgian Federal Science Policy Office; the Fonds pour la Formation à la Recherche dans l'Industrie et dans l'Agriculture (FRIA-Belgium); the Agentschap voor Innovatie door Wetenschap en Technologie (IWT-Belgium); the Ministry of Education, Youth and Sports (MEYS) of the Czech Republic; the Council of Science and Industrial Research, India; the HOMING PLUS program of the Foundation for Polish Science, cofinanced from European Union, Regional Development Fund, the Mobility Plus program of the Ministry of Science and Higher Education, the OPUS program contract 2014/13/B/ST2/02543 and contract Sonata-bis DEC-2012/07/E/ST2/01406 of the National Science Center (Poland); the Thalis and Aristeia programs cofinanced by EU-ESF and the Greek NSRF; the National Priorities Research Program by Qatar National Research Fund; the Programa Clarín-COFUND del Principado de Asturias; the Rachadapisek Sompot Fund for Postdoctoral Fellowship, Chulalongkorn University and the Chulalongkorn Academic into Its 2nd Century Project Advancement Project (Thailand); and the Welch Foundation, contract C-1845.

References

[1] CMS Collaboration, Observation of long-range near-side angular correlations in proton–proton collisions at the LHC, J. High Energy Phys. 09 (2010) 091, http://dx.doi.org/10.1007/JHEP09(2010)091, arXiv:1009.4122.

[2] ATLAS Collaboration, Observation of long-range elliptic azimuthal anisotropies in $\sqrt{s} = 13$ and 2.76 TeV pp collisions with the ATLAS detector, Phys. Rev. Lett. 116 (2016) 172301, http://dx.doi.org/10.1103/PhysRevLett.116.172301, arXiv:1509.04776.

[3] CMS Collaboration, Measurement of long-range near-side two-particle angular correlations in pp collisions at $\sqrt{s} = 13$ TeV, Phys. Rev. Lett. 116 (2016) 172302, http://dx.doi.org/10.1103/PhysRevLett.116.172302, arXiv:1510.03068.

[4] CMS Collaboration, Observation of long-range near-side angular correlations in proton–lead collisions at the LHC, Phys. Lett. B 718 (2013) 795, http://dx.doi.org/10.1016/j.physletb.2012.11.025, arXiv:1210.5482.

[5] ALICE Collaboration, Long-range angular correlations on the near and away side in pPb collisions at $\sqrt{s_{\rm NN}} = 5.02$ TeV, Phys. Lett. B 719 (2013) 29, http://dx.doi.org/10.1016/j.physletb.2013.01.012, arXiv:1212.2001.

[6] ATLAS Collaboration, Observation of associated near-side and away-side long-range correlations in $\sqrt{s_{NN}} = 5.02$ TeV proton–lead collisions with the ATLAS detector, Phys. Rev. Lett. 110 (2013) 182302, http://dx.doi.org/10.1103/PhysRevLett.110.182302, arXiv:1212.5198.

[7] LHCb Collaboration, Measurements of long-range near-side angular correlations in $\sqrt{s_{\rm NN}} = 5$ TeV proton–lead collisions in the forward region, arXiv:1512.00439, 2015.

[8] B. Alver, et al., PHOBOS, System size dependence of cluster properties from two-particle angular correlations in Cu+Cu and Au+Au collisions at $\sqrt{s_{\rm NN}} =$ 200 GeV, Phys. Rev. C 81 (2010) 024904, http://dx.doi.org/10.1103/PhysRevC.81.024904, arXiv:0812.1172.

[9] J. Adams, et al., STAR, Distributions of charged hadrons associated with high transverse momentum particles in pp and Au+Au collisions at $\sqrt{s_{\rm NN}} = 200$ GeV, Phys. Rev. Lett. 95 (2005) 152301, http://dx.doi.org/10.1103/PhysRevLett.95.152301, arXiv:nucl-ex/0501016.

[10] B.I. Abelev, et al., STAR, Long range rapidity correlations and jet production in high energy nuclear collisions, Phys. Rev. C 80 (2009) 064912, http://dx.doi.org/10.1103/PhysRevC.80.064912, arXiv:0909.0191.

[11] B. Alver, et al., PHOBOS, High transverse momentum triggered correlations over a large pseudorapidity acceptance in Au+Au collisions at $\sqrt{s_{\rm NN}} = 200$ GeV, Phys. Rev. Lett. 104 (2010) 062301, http://dx.doi.org/10.1103/PhysRevLett.104.062301, arXiv:0903.2811.

[12] B.I. Abelev, et al., STAR, Three-particle coincidence of the long range pseudorapidity correlation in high energy nucleus–nucleus collisions, Phys. Rev. Lett. 105 (2010) 022301, http://dx.doi.org/10.1103/PhysRevLett.105.022301, arXiv:0912.3977.

[13] CMS Collaboration, Long-range and short-range dihadron angular correlations in central PbPb collisions at a nucleon–nucleon center of mass energy of 2.76 TeV, J. High Energy Phys. 07 (2011) 076, http://dx.doi.org/10.1007/JHEP07(2011)076, arXiv:1105.2438.

[14] CMS Collaboration, Centrality dependence of dihadron correlations and azimuthal anisotropy harmonics in PbPb collisions at $\sqrt{s_{\rm NN}} = 2.76$ TeV, Eur. Phys. J. C 72 (2012) 2012, http://dx.doi.org/10.1140/epjc/s10052-012-2012-3, arXiv:1201.3158.

[15] ALICE Collaboration, Elliptic flow of charged particles in Pb–Pb collisions at 2.76 TeV, Phys. Rev. Lett. 105 (2010) 252302, http://dx.doi.org/10.1103/PhysRevLett.105.252302, arXiv:1011.3914.

[16] ATLAS Collaboration, Measurement of the azimuthal anisotropy for charged particle production in $\sqrt{s_{\rm NN}} = 2.76$ TeV lead–lead collisions with the ATLAS detector, Phys. Rev. C 86 (2012) 014907, http://dx.doi.org/10.1103/PhysRevC.86.014907, arXiv:1203.3087.

[17] CMS Collaboration, Measurement of the elliptic anisotropy of charged particles produced in PbPb collisions at nucleon–nucleon center-of-mass energy = 2.76 TeV, Phys. Rev. C 87 (2013) 014902, http://dx.doi.org/10.1103/PhysRevC.87.014902, arXiv:1204.1409.

[18] CMS Collaboration, Studies of azimuthal dihadron correlations in ultra-central PbPb collisions at $\sqrt{s_{\rm NN}} = 2.76$ TeV, J. High Energy Phys. 02 (2014) 088, http://dx.doi.org/10.1007/JHEP02(2014)088, arXiv:1312.1845.

[19] J.-Y. Ollitrault, Anisotropy as a signature of transverse collective flow, Phys. Rev. D 46 (1992) 229, http://dx.doi.org/10.1103/PhysRevD.46.229.

[20] U. Heinz, R. Snellings, Collective flow and viscosity in relativistic heavy-ion collisions, Annu. Rev. Nucl. Part. Sci. 63 (2013) 123, http://dx.doi.org/10.1146/annurev-nucl-102212-170540, arXiv:1301.2826.

[21] C. Gale, S. Jeon, B. Schenke, Hydrodynamic modeling of heavy-ion collisions, Int. J. Mod. Phys. A 28 (2013) 1340011, http://dx.doi.org/10.1142/S0217751X13400113, arXiv:1301.5893.

[22] S. Voloshin, Y. Zhang, Flow study in relativistic nuclear collisions by Fourier expansion of azimuthal particle distributions, Z. Phys. C 70 (1996) 665, http://dx.doi.org/10.1007/s002880050141, arXiv:hep-ph/9407282.

[23] B. Alver, G. Roland, Collision geometry fluctuations and triangular flow in heavy-ion collisions, Phys. Rev. C 81 (2010) 054905, http://dx.doi.org/10.1103/PhysRevC.81.054905, arXiv:1003.0194, erratum: http://dx.doi.org/10.1103/PhysRevC.82.039903.

[24] B.H. Alver, C. Gombeaud, M. Luzum, J.-Y. Ollitrault, Triangular flow in hydrodynamics and transport theory, Phys. Rev. C 82 (2010) 034913, http://dx.doi.org/10.1103/PhysRevC.82.034913, arXiv:1007.5469.

[25] B. Schenke, S. Jeon, C. Gale, Elliptic and triangular flow in event-by-event $D = 3 + 1$ viscous hydrodynamics, Phys. Rev. Lett. 106 (2011) 042301, http://dx.doi.org/10.1103/PhysRevLett.106.042301, arXiv:1009.3244.

[26] Z. Qiu, C. Shen, U. Heinz, Hydrodynamic elliptic and triangular flow in Pb–Pb collisions at $\sqrt{s_{\rm NN}} = 2.76$ TeV, Phys. Lett. B 707 (2012) 151, http://dx.doi.org/10.1016/j.physletb.2011.12.041, arXiv:1110.3033.

[27] A. Adare, et al., PHENIX, Measurement of long-range angular correlation and quadrupole anisotropy of pions and (anti)protons in central d+Au collisions at $\sqrt{s_{\rm NN}} = 200$ GeV, Phys. Rev. Lett. 114 (2015) 192301, http://dx.doi.org/10.1103/PhysRevLett.114.192301, arXiv:1404.7461.

[28] L. Adamczyk, et al., STAR, Long-range pseudorapidity dihadron correlations in d+Au collisions at $\sqrt{s_{\rm NN}} = 200$ GeV, Phys. Lett. B 747 (2015) 265, http://dx.doi.org/10.1016/j.physletb.2015.05.075, arXiv:1502.07652.

[29] A. Adare, et al., PHENIX, Measurements of elliptic and triangular flow in high-multiplicity ^{3}He+Au collisions at $\sqrt{s_{\rm NN}} = 200$ GeV, Phys. Rev. Lett. 115 (2015) 142301, http://dx.doi.org/10.1103/PhysRevLett.115.142301, arXiv:1507.06273.

[30] W. Li, Observation of a 'Ridge' correlation structure in high multiplicity proton–proton collisions: a brief review, Mod. Phys. Lett. A 27 (2012) 1230018, http://dx.doi.org/10.1142/S0217732312300182, arXiv:1206.0148.

[31] J.D. Bjorken, S.J. Brodsky, A. Scharff Goldhaber, Possible multiparticle ridge-like correlations in very high multiplicity proton–proton collisions, Phys. Lett. B 726 (2013) 344, http://dx.doi.org/10.1016/j.physletb.2013.08.066, arXiv:1308.1435.

[32] K. Dusling, W. Li, B. Schenke, Novel collective phenomena in high-energy proton–proton and proton–nucleus collisions, Int. J. Mod. Phys. E 25 (2016) 1630002, http://dx.doi.org/10.1142/S0218301316300022, arXiv:1509.07939.

[33] K. Dusling, R. Venugopalan, Explanation of systematics of CMS p+pb high multiplicity di-hadron data at $\sqrt{s_{\rm NN}} = 5.02$ TeV, Phys. Rev. D 87 (2013) 054014, http://dx.doi.org/10.1103/PhysRevD.87.054014, arXiv:1211.3701.

[34] K. Dusling, R. Venugopalan, Evidence for BFKL and saturation dynamics from dihadron spectra at the LHC, Phys. Rev. D 87 (2013) 051502, http://dx.doi.org/10.1103/PhysRevD.87.051502, arXiv:1210.3890.

[35] B. Schenke, R. Venugopalan, Eccentric protons? Sensitivity of flow to system size and shape in p+p, p+Pb and Pb+Pb collisions, Phys. Rev. Lett. 113 (2014) 102301, http://dx.doi.org/10.1103/PhysRevLett.113.102301, arXiv:1405.3605.

[36] P. Bozek, Collective flow in p–Pb and d–Pb collisions at TeV energies, Phys. Rev. C 85 (2012) 014911, http://dx.doi.org/10.1103/PhysRevC.85.014911, arXiv:1112.0915.
[37] P. Bozek, W. Broniowski, Correlations from hydrodynamic flow in pPb collisions, Phys. Lett. B 718 (2013) 1557, http://dx.doi.org/10.1016/j.physletb.2012.12.051, arXiv:1211.0845.
[38] ALICE Collaboration, Long-range angular correlations of pi, K and p in p–Pb collisions at $\sqrt{s_{\rm NN}} = 5.02$ TeV, Phys. Lett. B 726 (2013) 164, http://dx.doi.org/10.1016/j.physletb.2013.08.024, arXiv:1307.3237.
[39] CMS Collaboration, Long-range two-particle correlations of strange hadrons with charged particles in pPb and PbPb collisions at LHC energies, Phys. Lett. B 742 (2015) 200, http://dx.doi.org/10.1016/j.physletb.2015.01.034, arXiv:1409.3392.
[40] CMS Collaboration, Evidence for collective multi-particle correlations in pPb collisions, Phys. Rev. Lett. 115 (2015) 012301, http://dx.doi.org/10.1103/PhysRevLett.115.012301, arXiv:1502.05382.
[41] ALICE Collaboration, Multiparticle azimuthal correlations in p–Pb and Pb–Pb collisions at the CERN Large Hadron Collider, Phys. Rev. C 90 (2014) 054901, http://dx.doi.org/10.1103/PhysRevC.90.054901, arXiv:1406.2474.
[42] ATLAS Collaboration, Measurement with the ATLAS detector of multi-particle azimuthal correlations in p+Pb collisions at $\sqrt{s_{\rm NN}} = 5.02$ TeV, Phys. Lett. B 725 (2013) 60, http://dx.doi.org/10.1016/j.physletb.2013.06.057, arXiv:1303.2084.
[43] S. Chatrchyan, et al., CMS, Multiplicity and transverse momentum dependence of two- and four-particle correlations in pPb and PbPb collisions, Phys. Lett. B 724 (2013) 213, http://dx.doi.org/10.1016/j.physletb.2013.06.028, arXiv:1305.0609.
[44] K. Werner, M. Bleicher, B. Guiot, I. Karpenko, T. Pierog, Evidence for flow from hydrodynamic simulations of pPb collisions at 5.02 TeV from v_2 mass splitting, Phys. Rev. Lett. 112 (2014) 232301, http://dx.doi.org/10.1103/PhysRevLett.112.232301, arXiv:1307.4379.
[45] P. Bozek, W. Broniowski, G. Torrieri, Mass hierarchy in identified particle distributions in proton–lead collisions, Phys. Rev. Lett. 111 (2013) 172303, http://dx.doi.org/10.1103/PhysRevLett.111.172303, arXiv:1307.5060.
[46] L. Yan, J.-Y. Ollitrault, Universal fluctuation-driven eccentricities in proton–proton, proton–nucleus and nucleus–nucleus collisions, Phys. Rev. Lett. 112 (2014) 082301, http://dx.doi.org/10.1103/PhysRevLett.112.082301, arXiv:1312.6555.
[47] B. Schenke, S. Schlichting, P. Tribedy, R. Venugopalan, Mass ordering of spectra from fragmentation of saturated gluon states in high multiplicity proton–proton collisions, arXiv:1607.02496, 2016.
[48] CMS Collaboration, Description and performance of track and primary-vertex reconstruction with the CMS tracker, JINST 9 (2014) P10009, http://dx.doi.org/10.1088/1748-0221/9/10/P10009, arXiv:1405.6569.
[49] CMS Collaboration, The CMS experiment at the CERN LHC, JINST 3 (2008) S08004, http://dx.doi.org/10.1088/1748-0221/3/08/S08004.
[50] S. Agostinelli, et al., Geant4, Geant4—a simulation toolkit, Nucl. Instrum. Methods A 506 (2003) 250, http://dx.doi.org/10.1016/S0168-9002(03)01368-8.
[51] T. Sjöstrand, S. Mrenna, P. Skands, PYTHIA 6.4 physics and manual, J. High Energy Phys. 05 (2006) 026, http://dx.doi.org/10.1088/1126-6708/2006/05/026, arXiv:hep-ph/0603175.
[52] T. Sjöstrand, S. Mrenna, P. Skands, A brief introduction to PYTHIA 8.1, Comput. Phys. Commun. 178 (2008) 852, http://dx.doi.org/10.1016/j.cpc.2008.01.036, arXiv:0710.3820.
[53] CMS Collaboration, Strange particle production in pp collisions at $\sqrt{s} = 0.9$ and 7 TeV, J. High Energy Phys. 05 (2011) 064, http://dx.doi.org/10.1007/JHEP05(2011)064, arXiv:1102.4282.
[54] A. Bilandzic, R. Snellings, S. Voloshin, Flow analysis with cumulants: direct calculations, Phys. Rev. C 83 (2011) 044913, http://dx.doi.org/10.1103/PhysRevC.83.044913, arXiv:1010.0233.
[55] ALICE Collaboration, Harmonic decomposition of two-particle angular correlations in Pb–Pb collisions at $\sqrt{s_{\rm NN}} = 2.76$ TeV, Phys. Lett. B 708 (2012) 249, http://dx.doi.org/10.1016/j.physletb.2012.01.060, arXiv:1109.2501.
[56] ATLAS Collaboration, Measurement of long-range pseudorapidity correlations and azimuthal harmonics in $\sqrt{s_{NN}} = 5.02$ TeV proton–lead collisions with the ATLAS detector, Phys. Rev. C 90 (2014) 044906, http://dx.doi.org/10.1103/PhysRevC.90.044906, arXiv:1409.1792.
[57] G. Aad, et al., ATLAS, Measurement of the pseudorapidity and transverse momentum dependence of the elliptic flow of charged particles in lead–lead collisions at $\sqrt{s_{\rm NN}} = 2.76$ TeV with the ATLAS detector, Phys. Lett. B 707 (2012) 330, http://dx.doi.org/10.1016/j.physletb.2011.12.056, arXiv:1108.6018.
[58] ALICE Collaboration, Anisotropic flow of charged particles in Pb–Pb collisions at $\sqrt{s_{\rm NN}} = 5.02$ TeV, Phys. Rev. Lett. 116 (2016) 132302, http://dx.doi.org/10.1103/PhysRevLett.116.132302, arXiv:1602.01119.
[59] B.I. Abelev, et al., STAR, Mass, quark-number, and $\sqrt{s_{NN}}$ dependence of the second and fourth flow harmonics in ultra-relativistic nucleus–nucleus collisions, Phys. Rev. C 75 (2007) 054906, http://dx.doi.org/10.1103/PhysRevC.75.054906, arXiv:nucl-ex/0701010.
[60] A. Adare, et al., PHENIX, Deviation from quark-number scaling of the anisotropy parameter v_2 of pions, kaons, and protons in Au+Au collisions at $\sqrt{s_{\rm NN}} = 200$ GeV, Phys. Rev. C 85 (2012) 064914, http://dx.doi.org/10.1103/PhysRevC.85.064914, arXiv:1203.2644.
[61] N. Borghini, P.M. Dinh, J.-Y. Ollitrault, A new method for measuring azimuthal distributions in nucleus–nucleus collisions, Phys. Rev. C 63 (2001) 054906, http://dx.doi.org/10.1103/PhysRevC.63.054906, arXiv:nucl-th/0007063.
[62] G.J. Feldman, R.D. Cousins, A unified approach to the classical statistical analysis of small signals, Phys. Rev. D 57 (1998) 3873, http://dx.doi.org/10.1103/PhysRevD.57.3873, arXiv:physics/9711021.

CMS Collaboration

V. Khachatryan, A.M. Sirunyan, A. Tumasyan

Yerevan Physics Institute, Yerevan, Armenia

W. Adam, E. Asilar, T. Bergauer, J. Brandstetter, E. Brondolin, M. Dragicevic, J. Erö, M. Flechl, M. Friedl, R. Frühwirth [1], V.M. Ghete, C. Hartl, N. Hörmann, J. Hrubec, M. Jeitler [1], A. König, I. Krätschmer, D. Liko, T. Matsushita, I. Mikulec, D. Rabady, N. Rad, B. Rahbaran, H. Rohringer, J. Schieck [1], J. Strauss, W. Treberer-Treberspurg, W. Waltenberger, C.-E. Wulz [1]

Institut für Hochenergiephysik der OeAW, Wien, Austria

V. Mossolov, N. Shumeiko, J. Suarez Gonzalez

National Centre for Particle and High Energy Physics, Minsk, Belarus

S. Alderweireldt, E.A. De Wolf, X. Janssen, J. Lauwers, M. Van De Klundert, H. Van Haevermaet, P. Van Mechelen, N. Van Remortel, A. Van Spilbeeck

Universiteit Antwerpen, Antwerpen, Belgium

S. Abu Zeid, F. Blekman, J. D'Hondt, N. Daci, I. De Bruyn, K. Deroover, N. Heracleous, S. Lowette, S. Moortgat, L. Moreels, A. Olbrechts, Q. Python, S. Tavernier, W. Van Doninck, P. Van Mulders, I. Van Parijs

Vrije Universiteit Brussel, Brussel, Belgium

H. Brun, C. Caillol, B. Clerbaux, G. De Lentdecker, H. Delannoy, G. Fasanella, L. Favart, R. Goldouzian, A. Grebenyuk, G. Karapostoli, T. Lenzi, A. Léonard, J. Luetic, T. Maerschalk, A. Marinov, A. Randle-conde, T. Seva, C. Vander Velde, P. Vanlaer, R. Yonamine, F. Zenoni, F. Zhang [2]

Université Libre de Bruxelles, Bruxelles, Belgium

A. Cimmino, T. Cornelis, D. Dobur, A. Fagot, G. Garcia, M. Gul, D. Poyraz, S. Salva, R. Schöfbeck, A. Sharma, M. Tytgat, W. Van Driessche, E. Yazgan, N. Zaganidis

Ghent University, Ghent, Belgium

H. Bakhshiansohi, C. Beluffi [3], O. Bondu, S. Brochet, G. Bruno, A. Caudron, S. De Visscher, C. Delaere, M. Delcourt, B. Francois, A. Giammanco, A. Jafari, P. Jez, M. Komm, V. Lemaitre, A. Magitteri, A. Mertens, M. Musich, C. Nuttens, K. Piotrzkowski, L. Quertenmont, M. Selvaggi, M. Vidal Marono, S. Wertz

Université Catholique de Louvain, Louvain-la-Neuve, Belgium

N. Beliy

Université de Mons, Mons, Belgium

W.L. Aldá Júnior, F.L. Alves, G.A. Alves, L. Brito, C. Hensel, A. Moraes, M.E. Pol, P. Rebello Teles

Centro Brasileiro de Pesquisas Fisicas, Rio de Janeiro, Brazil

E. Belchior Batista Das Chagas, W. Carvalho, J. Chinellato [4], A. Custódio, E.M. Da Costa, G.G. Da Silveira [5], D. De Jesus Damiao, C. De Oliveira Martins, S. Fonseca De Souza, L.M. Huertas Guativa, H. Malbouisson, D. Matos Figueiredo, C. Mora Herrera, L. Mundim, H. Nogima, W.L. Prado Da Silva, A. Santoro, A. Sznajder, E.J. Tonelli Manganote [4], A. Vilela Pereira

Universidade do Estado do Rio de Janeiro, Rio de Janeiro, Brazil

S. Ahuja [a], C.A. Bernardes [b], S. Dogra [a], T.R. Fernandez Perez Tomei [a], E.M. Gregores [b], P.G. Mercadante [b], C.S. Moon [a], S.F. Novaes [a], Sandra S. Padula [a], D. Romero Abad [b], J.C. Ruiz Vargas

[a] *Universidade Estadual Paulista, São Paulo, Brazil*
[b] *Universidade Federal do ABC, São Paulo, Brazil*

A. Aleksandrov, R. Hadjiiska, P. Iaydjiev, M. Rodozov, S. Stoykova, G. Sultanov, M. Vutova

Institute for Nuclear Research and Nuclear Energy, Sofia, Bulgaria

A. Dimitrov, I. Glushkov, L. Litov, B. Pavlov, P. Petkov

University of Sofia, Sofia, Bulgaria

W. Fang [6]

Beihang University, Beijing, China

M. Ahmad, J.G. Bian, G.M. Chen, H.S. Chen, M. Chen, Y. Chen [7], T. Cheng, C.H. Jiang, D. Leggat, Z. Liu, F. Romeo, S.M. Shaheen, A. Spiezia, J. Tao, C. Wang, Z. Wang, H. Zhang, J. Zhao

Institute of High Energy Physics, Beijing, China

Y. Ban, G. Chen, Q. Li, S. Liu, Y. Mao, S.J. Qian, D. Wang, Z. Xu

State Key Laboratory of Nuclear Physics and Technology, Peking University, Beijing, China

C. Avila, A. Cabrera, L.F. Chaparro Sierra, C. Florez, J.P. Gomez, C.F. González Hernández, J.D. Ruiz Alvarez, J.C. Sanabria

Universidad de Los Andes, Bogota, Colombia

N. Godinovic, D. Lelas, I. Puljak, P.M. Ribeiro Cipriano, T. Sculac

University of Split, Faculty of Electrical Engineering, Mechanical Engineering and Naval Architecture, Split, Croatia

Z. Antunovic, M. Kovac

University of Split, Faculty of Science, Split, Croatia

V. Brigljevic, D. Ferencek, K. Kadija, S. Micanovic, L. Sudic, T. Susa

Institute Rudjer Boskovic, Zagreb, Croatia

A. Attikis, G. Mavromanolakis, J. Mousa, C. Nicolaou, F. Ptochos, P.A. Razis, H. Rykaczewski

University of Cyprus, Nicosia, Cyprus

M. Finger [8], M. Finger Jr. [8]

Charles University, Prague, Czechia

E. Carrera Jarrin

Universidad San Francisco de Quito, Quito, Ecuador

A.A. Abdelalim [9,10], E. El-khateeb [11], E. Salama [12,11]

Academy of Scientific Research and Technology of the Arab Republic of Egypt, Egyptian Network of High Energy Physics, Cairo, Egypt

B. Calpas, M. Kadastik, M. Murumaa, L. Perrini, M. Raidal, A. Tiko, C. Veelken

National Institute of Chemical Physics and Biophysics, Tallinn, Estonia

P. Eerola, J. Pekkanen, M. Voutilainen

Department of Physics, University of Helsinki, Helsinki, Finland

J. Härkönen, V. Karimäki, R. Kinnunen, T. Lampén, K. Lassila-Perini, S. Lehti, T. Lindén, P. Luukka, J. Tuominiemi, E. Tuovinen, L. Wendland

Helsinki Institute of Physics, Helsinki, Finland

J. Talvitie, T. Tuuva

Lappeenranta University of Technology, Lappeenranta, Finland

M. Besancon, F. Couderc, M. Dejardin, D. Denegri, B. Fabbro, J.L. Faure, C. Favaro, F. Ferri, S. Ganjour, S. Ghosh, A. Givernaud, P. Gras, G. Hamel de Monchenault, P. Jarry, I. Kucher, E. Locci, M. Machet, J. Malcles, J. Rander, A. Rosowsky, M. Titov, A. Zghiche

DSM/IRFU, CEA/Saclay, Gif-sur-Yvette, France

A. Abdulsalam, I. Antropov, S. Baffioni, F. Beaudette, P. Busson, L. Cadamuro, E. Chapon, C. Charlot, O. Davignon, R. Granier de Cassagnac, M. Jo, S. Lisniak, P. Miné, M. Nguyen, C. Ochando, G. Ortona, P. Paganini, P. Pigard, S. Regnard, R. Salerno, Y. Sirois, T. Strebler, Y. Yilmaz, A. Zabi

Laboratoire Leprince-Ringuet, Ecole Polytechnique, IN2P3-CNRS, Palaiseau, France

J.-L. Agram [13], J. Andrea, A. Aubin, D. Bloch, J.-M. Brom, M. Buttignol, E.C. Chabert, N. Chanon, C. Collard, E. Conte [13], X. Coubez, J.-C. Fontaine [13], D. Gelé, U. Goerlach, A.-C. Le Bihan, K. Skovpen, P. Van Hove

Institut Pluridisciplinaire Hubert Curien, Université de Strasbourg, Université de Haute Alsace Mulhouse, CNRS/IN2P3, Strasbourg, France

S. Gadrat

Centre de Calcul de l'Institut National de Physique Nucleaire et de Physique des Particules, CNRS/IN2P3, Villeurbanne, France

S. Beauceron, C. Bernet, G. Boudoul, E. Bouvier, C.A. Carrillo Montoya, R. Chierici, D. Contardo, B. Courbon, P. Depasse, H. El Mamouni, J. Fan, J. Fay, S. Gascon, M. Gouzevitch, G. Grenier, B. Ille, F. Lagarde, I.B. Laktineh, M. Lethuillier, L. Mirabito, A.L. Pequegnot, S. Perries, A. Popov [14], D. Sabes, V. Sordini, M. Vander Donckt, P. Verdier, S. Viret

Université de Lyon, Université Claude Bernard Lyon 1, CNRS-IN2P3, Institut de Physique Nucléaire de Lyon, Villeurbanne, France

T. Toriashvili [15]

Georgian Technical University, Tbilisi, Georgia

Z. Tsamalaidze [8]

Tbilisi State University, Tbilisi, Georgia

C. Autermann, S. Beranek, L. Feld, A. Heister, M.K. Kiesel, K. Klein, M. Lipinski, A. Ostapchuk, M. Preuten, F. Raupach, S. Schael, C. Schomakers, J.F. Schulte, J. Schulz, T. Verlage, H. Weber, V. Zhukov [14]

RWTH Aachen University, I. Physikalisches Institut, Aachen, Germany

A. Albert, M. Brodski, E. Dietz-Laursonn, D. Duchardt, M. Endres, M. Erdmann, S. Erdweg, T. Esch, R. Fischer, A. Güth, M. Hamer, T. Hebbeker, C. Heidemann, K. Hoepfner, S. Knutzen, M. Merschmeyer, A. Meyer, P. Millet, S. Mukherjee, M. Olschewski, K. Padeken, T. Pook, M. Radziej, H. Reithler, M. Rieger, F. Scheuch, L. Sonnenschein, D. Teyssier, S. Thüer

RWTH Aachen University, III. Physikalisches Institut A, Aachen, Germany

V. Cherepanov, G. Flügge, W. Haj Ahmad, F. Hoehle, B. Kargoll, T. Kress, A. Künsken, J. Lingemann, T. Müller, A. Nehrkorn, A. Nowack, I.M. Nugent, C. Pistone, O. Pooth, A. Stahl [16]

RWTH Aachen University, III. Physikalisches Institut B, Aachen, Germany

M. Aldaya Martin, C. Asawatangtrakuldee, K. Beernaert, O. Behnke, U. Behrens, A.A. Bin Anuar, K. Borras [17], A. Campbell, P. Connor, C. Contreras-Campana, F. Costanza, C. Diez Pardos, G. Dolinska, G. Eckerlin, D. Eckstein, E. Eren, E. Gallo [18], J. Garay Garcia, A. Geiser, A. Gizhko, J.M. Grados Luyando, P. Gunnellini, A. Harb, J. Hauk, M. Hempel [19], H. Jung, A. Kalogeropoulos, O. Karacheban [19], M. Kasemann, J. Keaveney, C. Kleinwort, I. Korol, D. Krücker, W. Lange, A. Lelek, J. Leonard, K. Lipka, A. Lobanov, W. Lohmann [19], R. Mankel, I.-A. Melzer-Pellmann, A.B. Meyer, G. Mittag, J. Mnich, A. Mussgiller, E. Ntomari, D. Pitzl, A. Raspereza, B. Roland, M.Ö. Sahin, P. Saxena, T. Schoerner-Sadenius, C. Seitz, S. Spannagel, N. Stefaniuk, G.P. Van Onsem, R. Walsh, C. Wissing

Deutsches Elektronen-Synchrotron, Hamburg, Germany

V. Blobel, M. Centis Vignali, A.R. Draeger, T. Dreyer, E. Garutti, D. Gonzalez, J. Haller, M. Hoffmann, A. Junkes, R. Klanner, R. Kogler, N. Kovalchuk, T. Lapsien, T. Lenz, I. Marchesini, D. Marconi, M. Meyer, M. Niedziela, D. Nowatschin, F. Pantaleo [16], T. Peiffer, A. Perieanu, J. Poehlsen, C. Sander, C. Scharf, P. Schleper, A. Schmidt, S. Schumann, J. Schwandt, H. Stadie, G. Steinbrück, F.M. Stober, M. Stöver, H. Tholen, D. Troendle, E. Usai, L. Vanelderen, A. Vanhoefer, B. Vormwald

University of Hamburg, Hamburg, Germany

C. Barth, C. Baus, J. Berger, E. Butz, T. Chwalek, F. Colombo, W. De Boer, A. Dierlamm, S. Fink, R. Friese, M. Giffels, A. Gilbert, P. Goldenzweig, D. Haitz, F. Hartmann [16], S.M. Heindl, U. Husemann, I. Katkov [14], P. Lobelle Pardo, B. Maier, H. Mildner, M.U. Mozer, Th. Müller, M. Plagge, G. Quast, K. Rabbertz, S. Röcker, F. Roscher, M. Schröder, I. Shvetsov, G. Sieber, H.J. Simonis, R. Ulrich, J. Wagner-Kuhr, S. Wayand, M. Weber, T. Weiler, S. Williamson, C. Wöhrmann, R. Wolf

Institut für Experimentelle Kernphysik, Karlsruhe, Germany

G. Anagnostou, G. Daskalakis, T. Geralis, V.A. Giakoumopoulou, A. Kyriakis, D. Loukas, I. Topsis-Giotis

Institute of Nuclear and Particle Physics (INPP), NCSR Demokritos, Aghia Paraskevi, Greece

S. Kesisoglou, A. Panagiotou, N. Saoulidou, E. Tziaferi

National and Kapodistrian University of Athens, Athens, Greece

I. Evangelou, G. Flouris, C. Foudas, P. Kokkas, N. Loukas, N. Manthos, I. Papadopoulos, E. Paradas

University of Ioánnina, Ioánnina, Greece

N. Filipovic

MTA-ELTE Lendület CMS Particle and Nuclear Physics Group, Eötvös Loránd University, Hungary

G. Bencze, C. Hajdu, P. Hidas, D. Horvath [20], F. Sikler, V. Veszpremi, G. Vesztergombi [21], A.J. Zsigmond

Wigner Research Centre for Physics, Budapest, Hungary

N. Beni, S. Czellar, J. Karancsi [22], A. Makovec, J. Molnar, Z. Szillasi

Institute of Nuclear Research ATOMKI, Debrecen, Hungary

M. Bartók [21], P. Raics, Z.L. Trocsanyi, B. Ujvari

University of Debrecen, Debrecen, Hungary

S. Bahinipati, S. Choudhury [23], P. Mal, K. Mandal, A. Nayak [24], D.K. Sahoo, N. Sahoo, S.K. Swain

National Institute of Science Education and Research, Bhubaneswar, India

S. Bansal, S.B. Beri, V. Bhatnagar, R. Chawla, U. Bhawandeep, A.K. Kalsi, A. Kaur, M. Kaur, R. Kumar, A. Mehta, M. Mittal, J.B. Singh, G. Walia

Panjab University, Chandigarh, India

Ashok Kumar, A. Bhardwaj, B.C. Choudhary, R.B. Garg, S. Keshri, S. Malhotra, M. Naimuddin, N. Nishu, K. Ranjan, R. Sharma, V. Sharma

University of Delhi, Delhi, India

R. Bhattacharya, S. Bhattacharya, K. Chatterjee, S. Dey, S. Dutt, S. Dutta, S. Ghosh, N. Majumdar, A. Modak, K. Mondal, S. Mukhopadhyay, S. Nandan, A. Purohit, A. Roy, D. Roy, S. Roy Chowdhury, S. Sarkar, M. Sharan, S. Thakur

Saha Institute of Nuclear Physics, Kolkata, India

P.K. Behera

Indian Institute of Technology Madras, Madras, India

R. Chudasama, D. Dutta, V. Jha, V. Kumar, A.K. Mohanty [16], P.K. Netrakanti, L.M. Pant, P. Shukla, A. Topkar

Bhabha Atomic Research Centre, Mumbai, India

T. Aziz, S. Dugad, G. Kole, B. Mahakud, S. Mitra, G.B. Mohanty, B. Parida, N. Sur, B. Sutar

Tata Institute of Fundamental Research-A, Mumbai, India

S. Banerjee, S. Bhowmik [25], R.K. Dewanjee, S. Ganguly, M. Guchait, Sa. Jain, S. Kumar, M. Maity [25], G. Majumder, K. Mazumdar, T. Sarkar [25], N. Wickramage [26]

Tata Institute of Fundamental Research-B, Mumbai, India

S. Chauhan, S. Dube, V. Hegde, A. Kapoor, K. Kothekar, A. Rane, S. Sharma

Indian Institute of Science Education and Research (IISER), Pune, India

H. Behnamian, S. Chenarani [27], E. Eskandari Tadavani, S.M. Etesami [27], A. Fahim [28], M. Khakzad, M. Mohammadi Najafabadi, M. Naseri, S. Paktinat Mehdiabadi [29], F. Rezaei Hosseinabadi, B. Safarzadeh [30], M. Zeinali

Institute for Research in Fundamental Sciences (IPM), Tehran, Iran

M. Felcini, M. Grunewald

University College Dublin, Dublin, Ireland

M. Abbrescia [a,b], C. Calabria [a,b], C. Caputo [a,b], A. Colaleo [a], D. Creanza [a,c], L. Cristella [a,b], N. De Filippis [a,c], M. De Palma [a,b], L. Fiore [a], G. Iaselli [a,c], G. Maggi [a,c], M. Maggi [a], G. Miniello [a,b], S. My [a,b], S. Nuzzo [a,b], A. Pompili [a,b], G. Pugliese [a,c], R. Radogna [a,b], A. Ranieri [a], G. Selvaggi [a,b], L. Silvestris [a,16], R. Venditti [a,b], P. Verwilligen [a]

[a] *INFN Sezione di Bari, Bari, Italy*
[b] *Università di Bari, Bari, Italy*
[c] *Politecnico di Bari, Bari, Italy*

G. Abbiendi [a], C. Battilana, D. Bonacorsi [a,b], S. Braibant-Giacomelli [a,b], L. Brigliadori [a,b], R. Campanini [a,b], P. Capiluppi [a,b], A. Castro [a,b], F.R. Cavallo [a], S.S. Chhibra [a,b], G. Codispoti [a,b], M. Cuffiani [a,b], G.M. Dallavalle [a], F. Fabbri [a], A. Fanfani [a,b], D. Fasanella [a,b], P. Giacomelli [a], C. Grandi [a], L. Guiducci [a,b], S. Marcellini [a], G. Masetti [a], A. Montanari [a], F.L. Navarria [a,b], A. Perrotta [a], A.M. Rossi [a,b], T. Rovelli [a,b], G.P. Siroli [a,b], N. Tosi [a,b,16]

[a] *INFN Sezione di Bologna, Bologna, Italy*
[b] *Università di Bologna, Bologna, Italy*

S. Albergo [a,b], M. Chiorboli [a,b], S. Costa [a,b], A. Di Mattia [a], F. Giordano [a,b], R. Potenza [a,b], A. Tricomi [a,b], C. Tuve [a,b]

[a] *INFN Sezione di Catania, Catania, Italy*
[b] *Università di Catania, Catania, Italy*

G. Barbagli [a], V. Ciulli [a,b], C. Civinini [a], R. D'Alessandro [a,b], E. Focardi [a,b], V. Gori [a,b], P. Lenzi [a,b], M. Meschini [a], S. Paoletti [a], G. Sguazzoni [a], L. Viliani [a,b,16]

[a] *INFN Sezione di Firenze, Firenze, Italy*
[b] *Università di Firenze, Firenze, Italy*

L. Benussi, S. Bianco, F. Fabbri, D. Piccolo, F. Primavera [16]

INFN Laboratori Nazionali di Frascati, Frascati, Italy

V. Calvelli [a,b], F. Ferro [a], M. Lo Vetere [a,b], M.R. Monge [a,b], E. Robutti [a], S. Tosi [a,b]

[a] *INFN Sezione di Genova, Genova, Italy*
[b] *Università di Genova, Genova, Italy*

L. Brianza [16], M.E. Dinardo [a,b], S. Fiorendi [a,b], S. Gennai [a], A. Ghezzi [a,b], P. Govoni [a,b], M. Malberti, S. Malvezzi [a], R.A. Manzoni [a,b,16], B. Marzocchi [a,b], D. Menasce [a], L. Moroni [a], M. Paganoni [a,b], D. Pedrini [a], S. Pigazzini, S. Ragazzi [a,b], T. Tabarelli de Fatis [a,b]

[a] *INFN Sezione di Milano-Bicocca, Milano, Italy*
[b] *Università di Milano-Bicocca, Milano, Italy*

S. Buontempo [a], N. Cavallo [a,c], G. De Nardo, S. Di Guida [a,d,16], M. Esposito [a,b], F. Fabozzi [a,c], A.O.M. Iorio [a,b], G. Lanza [a], L. Lista [a], S. Meola [a,d,16], P. Paolucci [a,16], C. Sciacca [a,b], F. Thyssen

[a] *INFN Sezione di Napoli, Napoli, Italy*
[b] *Università di Napoli 'Federico II', Napoli, Italy*

[c] Università della Basilicata, Potenza, Italy
[d] Università G. Marconi, Roma, Italy

P. Azzi [a,16], N. Bacchetta [a], L. Benato [a,b], D. Bisello [a,b], A. Boletti [a,b], R. Carlin [a,b], A. Carvalho Antunes De Oliveira [a,b], P. Checchia [a], M. Dall'Osso [a,b], P. De Castro Manzano [a], T. Dorigo [a], U. Dosselli [a], F. Gasparini [a,b], U. Gasparini [a,b], A. Gozzelino [a], S. Lacaprara [a], M. Margoni [a,b], A.T. Meneguzzo [a,b], J. Pazzini [a,b,16], N. Pozzobon [a,b], P. Ronchese [a,b], F. Simonetto [a,b], E. Torassa [a], M. Zanetti, P. Zotto [a,b], A. Zucchetta [a,b], G. Zumerle [a,b]

[a] INFN Sezione di Padova, Padova, Italy
[b] Università di Padova, Padova, Italy
[c] Università di Trento, Trento, Italy

A. Braghieri [a], A. Magnani [a,b], P. Montagna [a,b], S.P. Ratti [a,b], V. Re [a], C. Riccardi [a,b], P. Salvini [a], I. Vai [a,b], P. Vitulo [a,b]

[a] INFN Sezione di Pavia, Pavia, Italy
[b] Università di Pavia, Pavia, Italy

L. Alunni Solestizi [a,b], G.M. Bilei [a], D. Ciangottini [a,b], L. Fanò [a,b], P. Lariccia [a,b], R. Leonardi [a,b], G. Mantovani [a,b], M. Menichelli [a], A. Saha [a], A. Santocchia [a,b]

[a] INFN Sezione di Perugia, Perugia, Italy
[b] Università di Perugia, Perugia, Italy

K. Androsov [a,31], P. Azzurri [a,16], G. Bagliesi [a], J. Bernardini [a], T. Boccali [a], R. Castaldi [a], M.A. Ciocci [a,31], R. Dell'Orso [a], S. Donato [a,c], G. Fedi, A. Giassi [a], M.T. Grippo [a,31], F. Ligabue [a,c], T. Lomtadze [a], L. Martini [a,b], A. Messineo [a,b], F. Palla [a], A. Rizzi [a,b], A. Savoy-Navarro [a,32], P. Spagnolo [a], R. Tenchini [a], G. Tonelli [a,b], A. Venturi [a], P.G. Verdini [a]

[a] INFN Sezione di Pisa, Pisa, Italy
[b] Università di Pisa, Pisa, Italy
[c] Scuola Normale Superiore di Pisa, Pisa, Italy

L. Barone [a,b], F. Cavallari [a], M. Cipriani [a,b], G. D'imperio [a,b,16], D. Del Re [a,b,16], M. Diemoz [a], S. Gelli [a,b], E. Longo [a,b], F. Margaroli [a,b], P. Meridiani [a], G. Organtini [a,b], R. Paramatti [a], F. Preiato [a,b], S. Rahatlou [a,b], C. Rovelli [a], F. Santanastasio [a,b]

[a] INFN Sezione di Roma, Roma, Italy
[b] Università di Roma, Roma, Italy

N. Amapane [a,b], R. Arcidiacono [a,c,16], S. Argiro [a,b], M. Arneodo [a,c], N. Bartosik [a], R. Bellan [a,b], C. Biino [a], N. Cartiglia [a], F. Cenna [a,b], M. Costa [a,b], R. Covarelli [a,b], A. Degano [a,b], N. Demaria [a], L. Finco [a,b], B. Kiani [a,b], C. Mariotti [a], S. Maselli [a], E. Migliore [a,b], V. Monaco [a,b], E. Monteil [a,b], M.M. Obertino [a,b], L. Pacher [a,b], N. Pastrone [a], M. Pelliccioni [a], G.L. Pinna Angioni [a,b], F. Ravera [a,b], A. Romero [a,b], M. Ruspa [a,c], R. Sacchi [a,b], K. Shchelina [a,b], V. Sola [a], A. Solano [a,b], A. Staiano [a], P. Traczyk [a,b]

[a] INFN Sezione di Torino, Torino, Italy
[b] Università di Torino, Torino, Italy
[c] Università del Piemonte Orientale, Novara, Italy

S. Belforte [a], M. Casarsa [a], F. Cossutti [a], G. Della Ricca [a,b], C. La Licata [a,b], A. Schizzi [a,b], A. Zanetti [a]

[a] INFN Sezione di Trieste, Trieste, Italy
[b] Università di Trieste, Trieste, Italy

D.H. Kim, G.N. Kim, M.S. Kim, S. Lee, S.W. Lee, Y.D. Oh, S. Sekmen, D.C. Son, Y.C. Yang

Kyungpook National University, Daegu, Republic of Korea

A. Lee

Chonbuk National University, Jeonju, Republic of Korea

H. Kim

Chonnam National University, Institute for Universe and Elementary Particles, Kwangju, Republic of Korea

J.A. Brochero Cifuentes, T.J. Kim

Hanyang University, Seoul, Republic of Korea

S. Cho, S. Choi, Y. Go, D. Gyun, S. Ha, B. Hong, Y. Jo, Y. Kim, B. Lee, K. Lee, K.S. Lee, S. Lee, J. Lim, S.K. Park, Y. Roh

Korea University, Seoul, Republic of Korea

J. Almond, J. Kim, H. Lee, S.B. Oh, B.C. Radburn-Smith, S.h. Seo, U.K. Yang, H.D. Yoo, G.B. Yu

Seoul National University, Seoul, Republic of Korea

M. Choi, H. Kim, J.H. Kim, J.S.H. Lee, I.C. Park, G. Ryu, M.S. Ryu

University of Seoul, Seoul, Republic of Korea

Y. Choi, J. Goh, C. Hwang, J. Lee, I. Yu

Sungkyunkwan University, Suwon, Republic of Korea

V. Dudenas, A. Juodagalvis, J. Vaitkus

Vilnius University, Vilnius, Lithuania

I. Ahmed, Z.A. Ibrahim, J.R. Komaragiri, M.A.B. Md Ali [33], F. Mohamad Idris [34], W.A.T. Wan Abdullah, M.N. Yusli, Z. Zolkapli

National Centre for Particle Physics, Universiti Malaya, Kuala Lumpur, Malaysia

H. Castilla-Valdez, E. De La Cruz-Burelo, I. Heredia-De La Cruz [35], A. Hernandez-Almada, R. Lopez-Fernandez, R. Magaña Villalba, J. Mejia Guisao, A. Sanchez-Hernandez

Centro de Investigacion y de Estudios Avanzados del IPN, Mexico City, Mexico

S. Carrillo Moreno, C. Oropeza Barrera, F. Vazquez Valencia

Universidad Iberoamericana, Mexico City, Mexico

S. Carpinteyro, I. Pedraza, H.A. Salazar Ibarguen, C. Uribe Estrada

Benemerita Universidad Autonoma de Puebla, Puebla, Mexico

A. Morelos Pineda

Universidad Autónoma de San Luis Potosí, San Luis Potosí, Mexico

D. Krofcheck

University of Auckland, Auckland, New Zealand

P.H. Butler

University of Canterbury, Christchurch, New Zealand

A. Ahmad, M. Ahmad, Q. Hassan, H.R. Hoorani, W.A. Khan, M.A. Shah, M. Shoaib, M. Waqas

National Centre for Physics, Quaid-I-Azam University, Islamabad, Pakistan

H. Bialkowska, M. Bluj, B. Boimska, T. Frueboes, M. Górski, M. Kazana, K. Nawrocki, K. Romanowska-Rybinska, M. Szleper, P. Zalewski

National Centre for Nuclear Research, Swierk, Poland

K. Bunkowski, A. Byszuk [36], K. Doroba, A. Kalinowski, M. Konecki, J. Krolikowski, M. Misiura, M. Olszewski, M. Walczak

Institute of Experimental Physics, Faculty of Physics, University of Warsaw, Warsaw, Poland

P. Bargassa, C. Beirão Da Cruz E Silva, A. Di Francesco, P. Faccioli, P.G. Ferreira Parracho, M. Gallinaro, J. Hollar, N. Leonardo, L. Lloret Iglesias, M.V. Nemallapudi, J. Rodrigues Antunes, J. Seixas, O. Toldaiev, D. Vadruccio, J. Varela, P. Vischia

Laboratório de Instrumentação e Física Experimental de Partículas, Lisboa, Portugal

S. Afanasiev, P. Bunin, M. Gavrilenko, I. Golutvin, I. Gorbunov, A. Kamenev, V. Karjavin, A. Lanev, A. Malakhov, V. Matveev [37,38], P. Moisenz, V. Palichik, V. Perelygin, S. Shmatov, S. Shulha, N. Skatchkov, V. Smirnov, N. Voytishin, A. Zarubin

Joint Institute for Nuclear Research, Dubna, Russia

L. Chtchipounov, V. Golovtsov, Y. Ivanov, V. Kim [39], E. Kuznetsova [40], V. Murzin, V. Oreshkin, V. Sulimov, A. Vorobyev

Petersburg Nuclear Physics Institute, Gatchina (St. Petersburg), Russia

Yu. Andreev, A. Dermenev, S. Gninenko, N. Golubev, A. Karneyeu, M. Kirsanov, N. Krasnikov, A. Pashenkov, D. Tlisov, A. Toropin

Institute for Nuclear Research, Moscow, Russia

V. Epshteyn, V. Gavrilov, N. Lychkovskaya, V. Popov, I. Pozdnyakov, G. Safronov, A. Spiridonov, M. Toms, E. Vlasov, A. Zhokin

Institute for Theoretical and Experimental Physics, Moscow, Russia

A. Bylinkin [38]

MIPT, Russia

M. Chadeeva [41], R. Chistov [41], V. Rusinov

National Research Nuclear University, 'Moscow Engineering Physics Institute' (MEPhI), Moscow, Russia

V. Andreev, M. Azarkin [38], I. Dremin [38], M. Kirakosyan, A. Leonidov [38], S.V. Rusakov, A. Terkulov

P.N. Lebedev Physical Institute, Moscow, Russia

A. Baskakov, A. Belyaev, E. Boos, M. Dubinin [42], L. Dudko, A. Ershov, A. Gribushin, V. Klyukhin, O. Kodolova, I. Lokhtin, I. Miagkov, S. Obraztsov, S. Petrushanko, V. Savrin, A. Snigirev

Skobeltsyn Institute of Nuclear Physics, Lomonosov Moscow State University, Moscow, Russia

V. Blinov [43], Y. Skovpen [43]

Novosibirsk State University (NSU), Novosibirsk, Russia

I. Azhgirey, I. Bayshev, S. Bitioukov, D. Elumakhov, V. Kachanov, A. Kalinin, D. Konstantinov, V. Krychkine, V. Petrov, R. Ryutin, A. Sobol, S. Troshin, N. Tyurin, A. Uzunian, A. Volkov

State Research Center of Russian Federation, Institute for High Energy Physics, Protvino, Russia

P. Adzic [44], P. Cirkovic, D. Devetak, M. Dordevic, J. Milosevic, V. Rekovic

University of Belgrade, Faculty of Physics and Vinca Institute of Nuclear Sciences, Belgrade, Serbia

J. Alcaraz Maestre, M. Barrio Luna, E. Calvo, M. Cerrada, M. Chamizo Llatas, N. Colino, B. De La Cruz, A. Delgado Peris, A. Escalante Del Valle, C. Fernandez Bedoya, J.P. Fernández Ramos, J. Flix, M.C. Fouz,

P. Garcia-Abia, O. Gonzalez Lopez, S. Goy Lopez, J.M. Hernandez, M.I. Josa, E. Navarro De Martino, A. Pérez-Calero Yzquierdo, J. Puerta Pelayo, A. Quintario Olmeda, I. Redondo, L. Romero, M.S. Soares

Centro de Investigaciones Energéticas Medioambientales y Tecnológicas (CIEMAT), Madrid, Spain

J.F. de Trocóniz, M. Missiroli, D. Moran

Universidad Autónoma de Madrid, Madrid, Spain

J. Cuevas, J. Fernandez Menendez, I. Gonzalez Caballero, J.R. González Fernández, E. Palencia Cortezon, S. Sanchez Cruz, I. Suárez Andrés, J.M. Vizan Garcia

Universidad de Oviedo, Oviedo, Spain

I.J. Cabrillo, A. Calderon, J.R. Castiñeiras De Saa, E. Curras, M. Fernandez, J. Garcia-Ferrero, G. Gomez, A. Lopez Virto, J. Marco, C. Martinez Rivero, F. Matorras, J. Piedra Gomez, T. Rodrigo, A. Ruiz-Jimeno, L. Scodellaro, N. Trevisani, I. Vila, R. Vilar Cortabitarte

Instituto de Física de Cantabria (IFCA), CSIC-Universidad de Cantabria, Santander, Spain

D. Abbaneo, E. Auffray, G. Auzinger, M. Bachtis, P. Baillon, A.H. Ball, D. Barney, P. Bloch, A. Bocci, A. Bonato, C. Botta, T. Camporesi, R. Castello, M. Cepeda, G. Cerminara, M. D'Alfonso, D. d'Enterria, A. Dabrowski, V. Daponte, A. David, M. De Gruttola, A. De Roeck, E. Di Marco [45], M. Dobson, B. Dorney, T. du Pree, D. Duggan, M. Dünser, N. Dupont, A. Elliott-Peisert, S. Fartoukh, G. Franzoni, J. Fulcher, W. Funk, D. Gigi, K. Gill, M. Girone, F. Glege, D. Gulhan, S. Gundacker, M. Guthoff, J. Hammer, P. Harris, J. Hegeman, V. Innocente, P. Janot, J. Kieseler, H. Kirschenmann, V. Knünz, A. Kornmayer [16], M.J. Kortelainen, K. Kousouris, M. Krammer [1], C. Lange, P. Lecoq, C. Lourenço, M.T. Lucchini, L. Malgeri, M. Mannelli, A. Martelli, F. Meijers, J.A. Merlin, S. Mersi, E. Meschi, F. Moortgat, S. Morovic, M. Mulders, H. Neugebauer, S. Orfanelli, L. Orsini, L. Pape, E. Perez, M. Peruzzi, A. Petrilli, G. Petrucciani, A. Pfeiffer, M. Pierini, A. Racz, T. Reis, G. Rolandi [46], M. Rovere, M. Ruan, H. Sakulin, J.B. Sauvan, C. Schäfer, C. Schwick, M. Seidel, A. Sharma, P. Silva, P. Sphicas [47], J. Steggemann, M. Stoye, Y. Takahashi, M. Tosi, D. Treille, A. Triossi, A. Tsirou, V. Veckalns [48], G.I. Veres [21], N. Wardle, A. Zagozdzinska [36], W.D. Zeuner

CERN, European Organization for Nuclear Research, Geneva, Switzerland

W. Bertl, K. Deiters, W. Erdmann, R. Horisberger, Q. Ingram, H.C. Kaestli, D. Kotlinski, U. Langenegger, T. Rohe

Paul Scherrer Institut, Villigen, Switzerland

F. Bachmair, L. Bäni, L. Bianchini, B. Casal, G. Dissertori, M. Dittmar, M. Donegà, C. Grab, C. Heidegger, D. Hits, J. Hoss, G. Kasieczka, P. Lecomte †, W. Lustermann, B. Mangano, M. Marionneau, P. Martinez Ruiz del Arbol, M. Masciovecchio, M.T. Meinhard, D. Meister, F. Micheli, P. Musella, F. Nessi-Tedaldi, F. Pandolfi, J. Pata, F. Pauss, G. Perrin, L. Perrozzi, M. Quittnat, M. Rossini, M. Schönenberger, A. Starodumov [49], V.R. Tavolaro, K. Theofilatos, R. Wallny

Institute for Particle Physics, ETH Zurich, Zurich, Switzerland

T.K. Aarrestad, C. Amsler [50], L. Caminada, M.F. Canelli, A. De Cosa, C. Galloni, A. Hinzmann, T. Hreus, B. Kilminster, J. Ngadiuba, D. Pinna, G. Rauco, P. Robmann, D. Salerno, Y. Yang

Universität Zürich, Zurich, Switzerland

V. Candelise, T.H. Doan, Sh. Jain, R. Khurana, M. Konyushikhin, C.M. Kuo, W. Lin, Y.J. Lu, A. Pozdnyakov, S.S. Yu

National Central University, Chung-Li, Taiwan

Arun Kumar, P. Chang, Y.H. Chang, Y.W. Chang, Y. Chao, K.F. Chen, P.H. Chen, C. Dietz, F. Fiori, W.-S. Hou, Y. Hsiung, Y.F. Liu, R.-S. Lu, M. Miñano Moya, E. Paganis, A. Psallidas, J.f. Tsai, Y.M. Tzeng

National Taiwan University (NTU), Taipei, Taiwan

B. Asavapibhop, G. Singh, N. Srimanobhas, N. Suwonjandee

Chulalongkorn University, Faculty of Science, Department of Physics, Bangkok, Thailand

S. Cerci [51], S. Damarseckin, Z.S. Demiroglu, C. Dozen, I. Dumanoglu, S. Girgis, G. Gokbulut, Y. Guler, E. Gurpinar, I. Hos, E.E. Kangal [52], O. Kara, A. Kayis Topaksu, U. Kiminsu, M. Oglakci, G. Onengut [53], K. Ozdemir [54], D. Sunar Cerci [51], B. Tali [51], S. Turkcapar, I.S. Zorbakir, C. Zorbilmez

Cukurova University, Adana, Turkey

B. Bilin, S. Bilmis, B. Isildak [55], G. Karapinar [56], M. Yalvac, M. Zeyrek

Middle East Technical University, Physics Department, Ankara, Turkey

E. Gülmez, M. Kaya [57], O. Kaya [58], E.A. Yetkin [59], T. Yetkin [60]

Bogazici University, Istanbul, Turkey

A. Cakir, K. Cankocak, S. Sen [61]

Istanbul Technical University, Istanbul, Turkey

B. Grynyov

Institute for Scintillation Materials of National Academy of Science of Ukraine, Kharkov, Ukraine

L. Levchuk, P. Sorokin

National Scientific Center, Kharkov Institute of Physics and Technology, Kharkov, Ukraine

R. Aggleton, F. Ball, L. Beck, J.J. Brooke, D. Burns, E. Clement, D. Cussans, H. Flacher, J. Goldstein, M. Grimes, G.P. Heath, H.F. Heath, J. Jacob, L. Kreczko, C. Lucas, D.M. Newbold [62], S. Paramesvaran, A. Poll, T. Sakuma, S. Seif El Nasr-storey, D. Smith, V.J. Smith

University of Bristol, Bristol, United Kingdom

D. Barducci, A. Belyaev [63], C. Brew, R.M. Brown, L. Calligaris, D. Cieri, D.J.A. Cockerill, J.A. Coughlan, K. Harder, S. Harper, E. Olaiya, D. Petyt, C.H. Shepherd-Themistocleous, A. Thea, I.R. Tomalin, T. Williams

Rutherford Appleton Laboratory, Didcot, United Kingdom

M. Baber, R. Bainbridge, O. Buchmuller, A. Bundock, D. Burton, S. Casasso, M. Citron, D. Colling, L. Corpe, P. Dauncey, G. Davies, A. De Wit, M. Della Negra, R. Di Maria, P. Dunne, A. Elwood, D. Futyan, Y. Haddad, G. Hall, G. Iles, T. James, R. Lane, C. Laner, R. Lucas [62], L. Lyons, A.-M. Magnan, S. Malik, L. Mastrolorenzo, J. Nash, A. Nikitenko [49], J. Pela, B. Penning, M. Pesaresi, D.M. Raymond, A. Richards, A. Rose, C. Seez, S. Summers, A. Tapper, K. Uchida, M. Vazquez Acosta [64], T. Virdee [16], J. Wright, S.C. Zenz

Imperial College, London, United Kingdom

J.E. Cole, P.R. Hobson, A. Khan, P. Kyberd, D. Leslie, I.D. Reid, P. Symonds, L. Teodorescu, M. Turner

Brunel University, Uxbridge, United Kingdom

A. Borzou, K. Call, J. Dittmann, K. Hatakeyama, H. Liu, N. Pastika

Baylor University, Waco, USA

O. Charaf, S.I. Cooper, C. Henderson, P. Rumerio, C. West

The University of Alabama, Tuscaloosa, USA

D. Arcaro, A. Avetisyan, T. Bose, D. Gastler, D. Rankin, C. Richardson, J. Rohlf, L. Sulak, D. Zou

Boston University, Boston, USA

G. Benelli, E. Berry, D. Cutts, A. Garabedian, J. Hakala, U. Heintz, J.M. Hogan, O. Jesus, E. Laird, G. Landsberg, Z. Mao, M. Narain, S. Piperov, S. Sagir, E. Spencer, R. Syarif

Brown University, Providence, USA

R. Breedon, G. Breto, D. Burns, M. Calderon De La Barca Sanchez, S. Chauhan, M. Chertok, J. Conway, R. Conway, P.T. Cox, R. Erbacher, C. Flores, G. Funk, M. Gardner, W. Ko, R. Lander, C. Mclean, M. Mulhearn, D. Pellett, J. Pilot, S. Shalhout, J. Smith, M. Squires, D. Stolp, M. Tripathi, S. Wilbur, R. Yohay

University of California, Davis, Davis, USA

R. Cousins, P. Everaerts, A. Florent, J. Hauser, M. Ignatenko, D. Saltzberg, E. Takasugi, V. Valuev, M. Weber

University of California, Los Angeles, USA

K. Burt, R. Clare, J. Ellison, J.W. Gary, G. Hanson, J. Heilman, P. Jandir, E. Kennedy, F. Lacroix, O.R. Long, M. Olmedo Negrete, M.I. Paneva, A. Shrinivas, W. Si, H. Wei, S. Wimpenny, B.R. Yates

University of California, Riverside, Riverside, USA

J.G. Branson, G.B. Cerati, S. Cittolin, M. Derdzinski, R. Gerosa, A. Holzner, D. Klein, V. Krutelyov, J. Letts, I. Macneill, D. Olivito, S. Padhi, M. Pieri, M. Sani, V. Sharma, S. Simon, M. Tadel, A. Vartak, S. Wasserbaech [65], C. Welke, J. Wood, F. Würthwein, A. Yagil, G. Zevi Della Porta

University of California, San Diego, La Jolla, USA

R. Bhandari, J. Bradmiller-Feld, C. Campagnari, A. Dishaw, V. Dutta, K. Flowers, M. Franco Sevilla, P. Geffert, C. George, F. Golf, L. Gouskos, J. Gran, R. Heller, J. Incandela, N. Mccoll, S.D. Mullin, A. Ovcharova, J. Richman, D. Stuart, I. Suarez, J. Yoo

University of California, Santa Barbara, Santa Barbara, USA

D. Anderson, A. Apresyan, J. Bendavid, A. Bornheim, J. Bunn, Y. Chen, J. Duarte, J.M. Lawhorn, A. Mott, H.B. Newman, C. Pena, M. Spiropulu, J.R. Vlimant, S. Xie, R.Y. Zhu

California Institute of Technology, Pasadena, USA

M.B. Andrews, V. Azzolini, T. Ferguson, M. Paulini, J. Russ, M. Sun, H. Vogel, I. Vorobiev

Carnegie Mellon University, Pittsburgh, USA

J.P. Cumalat, W.T. Ford, F. Jensen, A. Johnson, M. Krohn, T. Mulholland, K. Stenson, S.R. Wagner

University of Colorado Boulder, Boulder, USA

J. Alexander, J. Chaves, J. Chu, S. Dittmer, K. Mcdermott, N. Mirman, G. Nicolas Kaufman, J.R. Patterson, A. Rinkevicius, A. Ryd, L. Skinnari, L. Soffi, S.M. Tan, Z. Tao, J. Thom, J. Tucker, P. Wittich, M. Zientek

Cornell University, Ithaca, USA

D. Winn

Fairfield University, Fairfield, USA

S. Abdullin, M. Albrow, G. Apollinari, S. Banerjee, L.A.T. Bauerdick, A. Beretvas, J. Berryhill, P.C. Bhat, G. Bolla, K. Burkett, J.N. Butler, H.W.K. Cheung, F. Chlebana, S. Cihangir [†], M. Cremonesi, V.D. Elvira, I. Fisk, J. Freeman, E. Gottschalk, L. Gray, D. Green, S. Grünendahl, O. Gutsche, D. Hare, R.M. Harris, S. Hasegawa, J. Hirschauer, Z. Hu, B. Jayatilaka, S. Jindariani, M. Johnson, U. Joshi, B. Klima, B. Kreis, S. Lammel, J. Linacre, D. Lincoln, R. Lipton, T. Liu, R. Lopes De Sá, J. Lykken, K. Maeshima, N. Magini, J.M. Marraffino, S. Maruyama, D. Mason, P. McBride, P. Merkel, S. Mrenna, S. Nahn, C. Newman-Holmes [†], V. O'Dell, K. Pedro, O. Prokofyev, G. Rakness, L. Ristori, E. Sexton-Kennedy, A. Soha, W.J. Spalding,

L. Spiegel, S. Stoynev, N. Strobbe, L. Taylor, S. Tkaczyk, N.V. Tran, L. Uplegger, E.W. Vaandering, C. Vernieri, M. Verzocchi, R. Vidal, M. Wang, H.A. Weber, A. Whitbeck

Fermi National Accelerator Laboratory, Batavia, USA

D. Acosta, P. Avery, P. Bortignon, D. Bourilkov, A. Brinkerhoff, A. Carnes, M. Carver, D. Curry, S. Das, R.D. Field, I.K. Furic, J. Konigsberg, A. Korytov, P. Ma, K. Matchev, H. Mei, P. Milenovic [66], G. Mitselmakher, D. Rank, L. Shchutska, D. Sperka, L. Thomas, J. Wang, S. Wang, J. Yelton

University of Florida, Gainesville, USA

S. Linn, P. Markowitz, G. Martinez, J.L. Rodriguez

Florida International University, Miami, USA

A. Ackert, J.R. Adams, T. Adams, A. Askew, S. Bein, B. Diamond, S. Hagopian, V. Hagopian, K.F. Johnson, A. Khatiwada, H. Prosper, A. Santra, M. Weinberg

Florida State University, Tallahassee, USA

M.M. Baarmand, V. Bhopatkar, S. Colafranceschi [67], M. Hohlmann, D. Noonan, T. Roy, F. Yumiceva

Florida Institute of Technology, Melbourne, USA

M.R. Adams, L. Apanasevich, D. Berry, R.R. Betts, I. Bucinskaite, R. Cavanaugh, O. Evdokimov, L. Gauthier, C.E. Gerber, D.J. Hofman, P. Kurt, C. O'Brien, I.D. Sandoval Gonzalez, P. Turner, N. Varelas, H. Wang, Z. Wu, M. Zakaria, J. Zhang

University of Illinois at Chicago (UIC), Chicago, USA

B. Bilki [68], W. Clarida, K. Dilsiz, S. Durgut, R.P. Gandrajula, M. Haytmyradov, V. Khristenko, J.-P. Merlo, H. Mermerkaya [69], A. Mestvirishvili, A. Moeller, J. Nachtman, H. Ogul, Y. Onel, F. Ozok [70], A. Penzo, C. Snyder, E. Tiras, J. Wetzel, K. Yi

The University of Iowa, Iowa City, USA

I. Anderson, B. Blumenfeld, A. Cocoros, N. Eminizer, D. Fehling, L. Feng, A.V. Gritsan, P. Maksimovic, M. Osherson, J. Roskes, U. Sarica, M. Swartz, M. Xiao, Y. Xin, C. You

Johns Hopkins University, Baltimore, USA

A. Al-bataineh, P. Baringer, A. Bean, S. Boren, J. Bowen, C. Bruner, J. Castle, L. Forthomme, R.P. Kenny III, A. Kropivnitskaya, D. Majumder, W. Mcbrayer, M. Murray, S. Sanders, R. Stringer, J.D. Tapia Takaki, Q. Wang

The University of Kansas, Lawrence, USA

A. Ivanov, K. Kaadze, S. Khalil, Y. Maravin, A. Mohammadi, L.K. Saini, N. Skhirtladze, S. Toda

Kansas State University, Manhattan, USA

F. Rebassoo, D. Wright

Lawrence Livermore National Laboratory, Livermore, USA

C. Anelli, A. Baden, O. Baron, A. Belloni, B. Calvert, S.C. Eno, C. Ferraioli, J.A. Gomez, N.J. Hadley, S. Jabeen, R.G. Kellogg, T. Kolberg, J. Kunkle, Y. Lu, A.C. Mignerey, F. Ricci-Tam, Y.H. Shin, A. Skuja, M.B. Tonjes, S.C. Tonwar

University of Maryland, College Park, USA

D. Abercrombie, B. Allen, A. Apyan, R. Barbieri, A. Baty, R. Bi, K. Bierwagen, S. Brandt, W. Busza, I.A. Cali, Z. Demiragli, L. Di Matteo, G. Gomez Ceballos, M. Goncharov, D. Hsu, Y. Iiyama, G.M. Innocenti, M. Klute,

D. Kovalskyi, K. Krajczar, Y.S. Lai, Y.-J. Lee, A. Levin, P.D. Luckey, A.C. Marini, C. Mcginn, C. Mironov, S. Narayanan, X. Niu, C. Paus, C. Roland, G. Roland, J. Salfeld-Nebgen, G.S.F. Stephans, K. Sumorok, K. Tatar, M. Varma, D. Velicanu, J. Veverka, J. Wang, T.W. Wang, B. Wyslouch, M. Yang, V. Zhukova

Massachusetts Institute of Technology, Cambridge, USA

A.C. Benvenuti, R.M. Chatterjee, A. Evans, A. Finkel, A. Gude, P. Hansen, S. Kalafut, S.C. Kao, Y. Kubota, Z. Lesko, J. Mans, S. Nourbakhsh, N. Ruckstuhl, R. Rusack, N. Tambe, J. Turkewitz

University of Minnesota, Minneapolis, USA

J.G. Acosta, S. Oliveros

University of Mississippi, Oxford, USA

E. Avdeeva, R. Bartek, K. Bloom, D.R. Claes, A. Dominguez, C. Fangmeier, R. Gonzalez Suarez, R. Kamalieddin, I. Kravchenko, A. Malta Rodrigues, F. Meier, J. Monroy, J.E. Siado, G.R. Snow, B. Stieger

University of Nebraska-Lincoln, Lincoln, USA

M. Alyari, J. Dolen, J. George, A. Godshalk, C. Harrington, I. Iashvili, J. Kaisen, A. Kharchilava, A. Kumar, A. Parker, S. Rappoccio, B. Roozbahani

State University of New York at Buffalo, Buffalo, USA

G. Alverson, E. Barberis, D. Baumgartel, A. Hortiangtham, A. Massironi, D.M. Morse, D. Nash, T. Orimoto, R. Teixeira De Lima, D. Trocino, R.-J. Wang, D. Wood

Northeastern University, Boston, USA

S. Bhattacharya, K.A. Hahn, A. Kubik, A. Kumar, J.F. Low, N. Mucia, N. Odell, B. Pollack, M.H. Schmitt, K. Sung, M. Trovato, M. Velasco

Northwestern University, Evanston, USA

N. Dev, M. Hildreth, K. Hurtado Anampa, C. Jessop, D.J. Karmgard, N. Kellams, K. Lannon, N. Marinelli, F. Meng, C. Mueller, Y. Musienko [37], M. Planer, A. Reinsvold, R. Ruchti, G. Smith, S. Taroni, M. Wayne, M. Wolf, A. Woodard

University of Notre Dame, Notre Dame, USA

J. Alimena, L. Antonelli, J. Brinson, B. Bylsma, L.S. Durkin, S. Flowers, B. Francis, A. Hart, C. Hill, R. Hughes, W. Ji, B. Liu, W. Luo, D. Puigh, B.L. Winer, H.W. Wulsin

The Ohio State University, Columbus, USA

S. Cooperstein, O. Driga, P. Elmer, J. Hardenbrook, P. Hebda, D. Lange, J. Luo, D. Marlow, T. Medvedeva, K. Mei, M. Mooney, J. Olsen, C. Palmer, P. Piroué, D. Stickland, C. Tully, A. Zuranski

Princeton University, Princeton, USA

S. Malik

University of Puerto Rico, Mayaguez, USA

A. Barker, V.E. Barnes, S. Folgueras, L. Gutay, M.K. Jha, M. Jones, A.W. Jung, K. Jung, D.H. Miller, N. Neumeister, X. Shi, J. Sun, A. Svyatkovskiy, F. Wang, W. Xie, L. Xu

Purdue University, West Lafayette, USA

N. Parashar, J. Stupak

Purdue University Calumet, Hammond, USA

A. Adair, B. Akgun, Z. Chen, K.M. Ecklund, F.J.M. Geurts, M. Guilbaud, W. Li, B. Michlin, M. Northup, B.P. Padley, R. Redjimi, J. Roberts, J. Rorie, Z. Tu, J. Zabel

Rice University, Houston, USA

B. Betchart, A. Bodek, P. de Barbaro, R. Demina, Y.t. Duh, T. Ferbel, M. Galanti, A. Garcia-Bellido, J. Han, O. Hindrichs, A. Khukhunaishvili, K.H. Lo, P. Tan, M. Verzetti

University of Rochester, Rochester, USA

A. Agapitos, J.P. Chou, E. Contreras-Campana, Y. Gershtein, T.A. Gómez Espinosa, E. Halkiadakis, M. Heindl, D. Hidas, E. Hughes, S. Kaplan, R. Kunnawalkam Elayavalli, S. Kyriacou, A. Lath, K. Nash, H. Saka, S. Salur, S. Schnetzer, D. Sheffield, S. Somalwar, R. Stone, S. Thomas, P. Thomassen, M. Walker

Rutgers, The State University of New Jersey, Piscataway, USA

M. Foerster, J. Heideman, G. Riley, K. Rose, S. Spanier, K. Thapa

University of Tennessee, Knoxville, USA

O. Bouhali [71], A. Celik, M. Dalchenko, M. De Mattia, A. Delgado, S. Dildick, R. Eusebi, J. Gilmore, T. Huang, E. Juska, T. Kamon [72], R. Mueller, Y. Pakhotin, R. Patel, A. Perloff, L. Perniè, D. Rathjens, A. Rose, A. Safonov, A. Tatarinov, K.A. Ulmer

Texas A&M University, College Station, USA

N. Akchurin, C. Cowden, J. Damgov, F. De Guio, C. Dragoiu, P.R. Dudero, J. Faulkner, S. Kunori, K. Lamichhane, S.W. Lee, T. Libeiro, T. Peltola, S. Undleeb, I. Volobouev, Z. Wang

Texas Tech University, Lubbock, USA

A.G. Delannoy, S. Greene, A. Gurrola, R. Janjam, W. Johns, C. Maguire, A. Melo, H. Ni, P. Sheldon, S. Tuo, J. Velkovska, Q. Xu

Vanderbilt University, Nashville, USA

M.W. Arenton, P. Barria, B. Cox, J. Goodell, R. Hirosky, A. Ledovskoy, H. Li, C. Neu, T. Sinthuprasith, X. Sun, Y. Wang, E. Wolfe, F. Xia

University of Virginia, Charlottesville, USA

C. Clarke, R. Harr, P.E. Karchin, P. Lamichhane, J. Sturdy

Wayne State University, Detroit, USA

D.A. Belknap, S. Dasu, L. Dodd, S. Duric, B. Gomber, M. Grothe, M. Herndon, A. Hervé, P. Klabbers, A. Lanaro, A. Levine, K. Long, R. Loveless, I. Ojalvo, T. Perry, G. Polese, T. Ruggles, A. Savin, N. Smith, W.H. Smith, D. Taylor, N. Woods

University of Wisconsin – Madison, Madison, WI, USA

† Deceased.
[1] Also at Vienna University of Technology, Vienna, Austria.
[2] Also at State Key Laboratory of Nuclear Physics and Technology, Peking University, Beijing, China.
[3] Also at Institut Pluridisciplinaire Hubert Curien, Université de Strasbourg, Université de Haute Alsace Mulhouse, CNRS/IN2P3, Strasbourg, France.
[4] Also at Universidade Estadual de Campinas, Campinas, Brazil.
[5] Also at Universidade Federal de Pelotas, Pelotas, Brazil.
[6] Also at Université Libre de Bruxelles, Bruxelles, Belgium.
[7] Also at Deutsches Elektronen-Synchrotron, Hamburg, Germany.
[8] Also at Joint Institute for Nuclear Research, Dubna, Russia.
[9] Also at Helwan University, Cairo, Egypt.
[10] Now at Zewail City of Science and Technology, Zewail, Egypt.
[11] Also at Ain Shams University, Cairo, Egypt.
[12] Also at British University in Egypt, Cairo, Egypt.
[13] Also at Université de Haute Alsace, Mulhouse, France.

[14] Also at Skobeltsyn Institute of Nuclear Physics, Lomonosov Moscow State University, Moscow, Russia.
[15] Also at Tbilisi State University, Tbilisi, Georgia.
[16] Also at CERN, European Organization for Nuclear Research, Geneva, Switzerland.
[17] Also at RWTH Aachen University, III. Physikalisches Institut A, Aachen, Germany.
[18] Also at University of Hamburg, Hamburg, Germany.
[19] Also at Brandenburg University of Technology, Cottbus, Germany.
[20] Also at Institute of Nuclear Research ATOMKI, Debrecen, Hungary.
[21] Also at MTA-ELTE Lendület CMS Particle and Nuclear Physics Group, Eötvös Loránd University, Budapest, Hungary.
[22] Also at University of Debrecen, Debrecen, Hungary.
[23] Also at Indian Institute of Science Education and Research, Bhopal, India.
[24] Also at Institute of Physics, Bhubaneswar, India.
[25] Also at University of Visva-Bharati, Santiniketan, India.
[26] Also at University of Ruhuna, Matara, Sri Lanka.
[27] Also at Isfahan University of Technology, Isfahan, Iran.
[28] Also at University of Tehran, Department of Engineering Science, Tehran, Iran.
[29] Also at Yazd University, Yazd, Iran.
[30] Also at Plasma Physics Research Center, Science and Research Branch, Islamic Azad University, Tehran, Iran.
[31] Also at Università degli Studi di Siena, Siena, Italy.
[32] Also at Purdue University, West Lafayette, USA.
[33] Also at International Islamic University of Malaysia, Kuala Lumpur, Malaysia.
[34] Also at Malaysian Nuclear Agency, MOSTI, Kajang, Malaysia.
[35] Also at Consejo Nacional de Ciencia y Tecnología, Mexico city, Mexico.
[36] Also at Warsaw University of Technology, Institute of Electronic Systems, Warsaw, Poland.
[37] Also at Institute for Nuclear Research, Moscow, Russia.
[38] Now at National Research Nuclear University 'Moscow Engineering Physics Institute' (MEPhI), Moscow, Russia.
[39] Also at St. Petersburg State Polytechnical University, St. Petersburg, Russia.
[40] Also at University of Florida, Gainesville, USA.
[41] Also at P.N. Lebedev Physical Institute, Moscow, Russia.
[42] Also at California Institute of Technology, Pasadena, USA.
[43] Also at Budker Institute of Nuclear Physics, Novosibirsk, Russia.
[44] Also at Faculty of Physics, University of Belgrade, Belgrade, Serbia.
[45] Also at INFN Sezione di Roma; Università di Roma, Roma, Italy.
[46] Also at Scuola Normale e Sezione dell'INFN, Pisa, Italy.
[47] Also at National and Kapodistrian University of Athens, Athens, Greece.
[48] Also at Riga Technical University, Riga, Latvia.
[49] Also at Institute for Theoretical and Experimental Physics, Moscow, Russia.
[50] Also at Albert Einstein Center for Fundamental Physics, Bern, Switzerland.
[51] Also at Adiyaman University, Adiyaman, Turkey.
[52] Also at Mersin University, Mersin, Turkey.
[53] Also at Cag University, Mersin, Turkey.
[54] Also at Piri Reis University, Istanbul, Turkey.
[55] Also at Ozyegin University, Istanbul, Turkey.
[56] Also at Izmir Institute of Technology, Izmir, Turkey.
[57] Also at Marmara University, Istanbul, Turkey.
[58] Also at Kafkas University, Kars, Turkey.
[59] Also at Istanbul Bilgi University, Istanbul, Turkey.
[60] Also at Yildiz Technical University, Istanbul, Turkey.
[61] Also at Hacettepe University, Ankara, Turkey.
[62] Also at Rutherford Appleton Laboratory, Didcot, United Kingdom.
[63] Also at School of Physics and Astronomy, University of Southampton, Southampton, United Kingdom.
[64] Also at Instituto de Astrofísica de Canarias, La Laguna, Spain.
[65] Also at Utah Valley University, Orem, USA.
[66] Also at University of Belgrade, Faculty of Physics and Vinca Institute of Nuclear Sciences, Belgrade, Serbia.
[67] Also at Facoltà Ingegneria, Università di Roma, Roma, Italy.
[68] Also at Argonne National Laboratory, Argonne, USA.
[69] Also at Erzincan University, Erzincan, Turkey.
[70] Also at Mimar Sinan University, Istanbul, Istanbul, Turkey.
[71] Also at Texas A&M University at Qatar, Doha, Qatar.
[72] Also at Kyungpook National University, Daegu, Republic of Korea.